



You have downloaded a document from
RE-BUŚ
repository of the University of Silesia in Katowice

Title: Distribution of Some Ecotoxic Elements in Fuel and Solid Combustion Residues in Poland

Author: Henryk R. Parzenty, Leokadia Róg

Citation style: Parzenty Henryk R., Róg Leokadia. (2020). Distribution of Some Ecotoxic Elements in Fuel and Solid Combustion Residues in Poland. "Energies" Vol. 13, iss. 5 (2020), art. no 1131, doi 10.3390/en13051131



Uznanie autorstwa - Licencja ta pozwala na kopiowanie, zmienianie, rozprowadzanie, przedstawianie i wykonywanie utworu jedynie pod warunkiem oznaczenia autorstwa.



UNIwersYTET ŚLĄSKI
W KATOWICACH




Biblioteka
Uniwersytetu Śląskiego



Ministerstwo Nauki
i Szkolnictwa Wyższego

Article

Distribution of Some Ecotoxic Elements in Fuel and Solid Combustion Residues in Poland

Henryk R. Parzenty ^{1,*}  and Leokadia Róg ²

¹ Active Non-Permanent Staff Member of the Institute of Earth Sciences, University of Silesia in Katowice, 41200 Sosnowiec, Poland

² Department of Solid Fuels Quality Assessment, Central Mining Institute, 40166 Katowice, Poland; Irog@gig.eu

* Correspondence: hr.parzenty@vp.pl

Received: 14 January 2020; Accepted: 26 February 2020; Published: 3 March 2020



Abstract: The purpose of this paper is to assess the content and distribution of some elements in coal from two bituminous coal basins and in fly ash and slag derived from combustion of the coals in six power plants in Poland. The petrographic composition and distribution of elements were characterized in the tested samples, using reflected light microscope, X-ray powder diffractometer, inductively coupled plasma atomic emission spectroscopy, and scanning electron microscope with energy dispersive X-ray. The highest content of elements in coal occurs in siderite. In Al-Si particles, as well as in magnetite with skeletal and dendritic structure crystallized on the surface of Al-Si microspheres or cenospheres included in fly ash size < 0.05 mm and in the magnetic fraction of slag, the highest content of elements was noted. Due to the content of elements, fly ash and slag were considered to be neutral for the soil environment. Correlations, which have not been described before, have been observed between the likely mode of binding of some elements in coal and their distribution in fly ash and slag. These correlations could be of particular value when predicting the content and distribution of elements in combustion residues and in the assessment of their environmental toxicity.

Keywords: bituminous coal; fly ash; slag; trace elements; power station

1. Introduction

The great interest in combustion waste from coal combustion in a power station (PS) results from both the wide range of its economic application and the fear of the possibility of environmental pollution. Hazard to the environment are both particulate matter, which obstructs breathing and settle in lungs, and trace elements contained in fly ash and slag. Radioactive and heavy elements are considered to be the most toxic to the environment [1–6], named by Duffus [7] as ecotoxic elements (EE).

Knowledge of the content and distribution of EE in coal may facilitate, among others things, determination of enrichment or depletion of these elements in fly ash, slag/bottom ash, and coal pyrolysis products; it may also facilitate the forecasting of EE leaching efficiency from coal, from mineral overgrowth of coal and from solid coal combustion products. It also has a significant impact on the behavior of elements during coal enrichment, conversion, and weathering [8–16]. It is assumed that, during the combustion of coal, the elements bound in coal mainly with the organic and sulfide fraction first evaporate, and then they easily adsorb on fine particles during the cooling of the flue gas. The opposite is true for elements combined with minerals other than sulfides, in which case they probably remain in the ash matrix or evaporate slowly [12,14,17–22]. The volatility of elements is variable, i.e., different in the initial and different in the main stage of coal combustion in TPS. This variability for each element in different modes of occurrence depends on the type of coal and operating conditions and especially on the combustion temperature [15,23–25]. The enrichment factor

of elements with high volatility, such as As, Hg, and Zn, are minimal for fly and bottom ash, indicating that these elements have escaped into the atmosphere with flue gas [8,14,24,26–28]. In addition, the removal of toxic elements by gradual release and acid leaching is also closely related to their occurrence. It is considered that most thiophilic and siderophilic elements have higher removability than lithophilic elements [6,29–32].

There is a justified need to verify the current observations regarding the assessment of the content and mode of binding of EE in coal feeds and in the residues after their combustion. There is also a need to look for the relationship between the way EE binding occurs in coal feeds, and its content and distribution in furnace waste generated in various power plants, for coal extracted from various basins. Changes in fuel quality affect, among others things, the instability of the chemical composition of the resulting fly ash and slag, and thus also the different efficiency of enrichment, extraction, and possible recovery of rare earth elements and other valuable elements [33–37]. Identifying the distribution of elements between products of the coal combustion process is necessary to develop effective methods to reduce their emissions into the environment. Therefore, the purpose of this paper is to evaluate the content and distribution of some EEs in feed coal, fly ash, and slag resulting from the combustion of bituminous feed coal in Poland. An attempt was made in this paper to find a relationship between the content and mode of binding EE in coal feeds, and the content and distribution of elements in fly ash and slag. The research covered the EE most frequently determined, most abundant, and most frequently occurring EE in coal and solid combustion waste from Poland (e.g., [38–41]). The assessment of distribution in coal and combustion waste of elements most dangerous for the environment, e.g., Hg, Th, Tl, and U are separate studies [42,43]. Feed coal came from the two largest bituminous coal basins in Poland, i.e., from the Lublin Coal Basin (LCB) and the Upper Silesian Coal Basin (USCB).

2. Materials and Methods

The subject of the study was feed coals originating from the LCB and the USCB and a permanent residue after the combustion of these feeds at power plants in Poland, i.e., fly ash and slag. Coal feeds were burned in dust, steam, and drum boilers, with a tangential furnace, at an average temperature of 1280 °C. The wet flue-gas desulphurization methods used in the boilers did not allow contact between the fly ash and slag with the sorbent. The location of the coal basins (the LCB and the USCB) and PS in Poland is shown in Figure 1 (see Supplementary Materials Table S1). The research involved the following:

- (1) Six samples of the LCB feed coals, six fly ash samples, and six slag samples resulting from the combustion of feed coal in two PS (the condition of the samples as received);
- (2) Seven samples of the USCB feed coals, seven fly ash samples, and seven slag samples resulting from the combustion of feed coal in six PS (the condition of the samples as received).

Samples of feeds coal (as received) were taken from the feeder to the boiler, immediately before its combustion. Fly ash samples were taken from electrostatic precipitators, and the slag samples were taken directly from the slag scrapers.

The petrographic composition and coal reflectivity were determined, using a Zeiss Axio Imager D1m microscope (40× objective, 10× oculars, and 546-nm interference filters, white-light reflected, immersion oil), with an integration table, in accordance with the standards defined by the International Committee for Coal and Organic Petrology and the procedures described in ISO 7404-3 [44] and PN-ISO 7404-5 [45]. The mineral composition of the mineral matter of the coal feed, verified by Bunker D8 Discover X-ray powder diffractometer (iron-filtered CoK α radiation, Ni-filter, and Lynxeye detector). The XRD pattern was recorded with an interval of 2θ 2.6°–70°, in increments of 0.01°. Calculations of the content of individual mineral phases were performed, using Diffrac v. 3.0 Bruker AXS software and commercial methodology developed by Taylor [46], based on the principles for diffractogram profiling defined by Rietveld [47]. The implementation of this method for carbon-containing materials

was presented by Ruan and Ward [48] and Mahieux et al. [49]. The results are shown in Table 1 (see Supplementary Materials Tables S2 and S3).

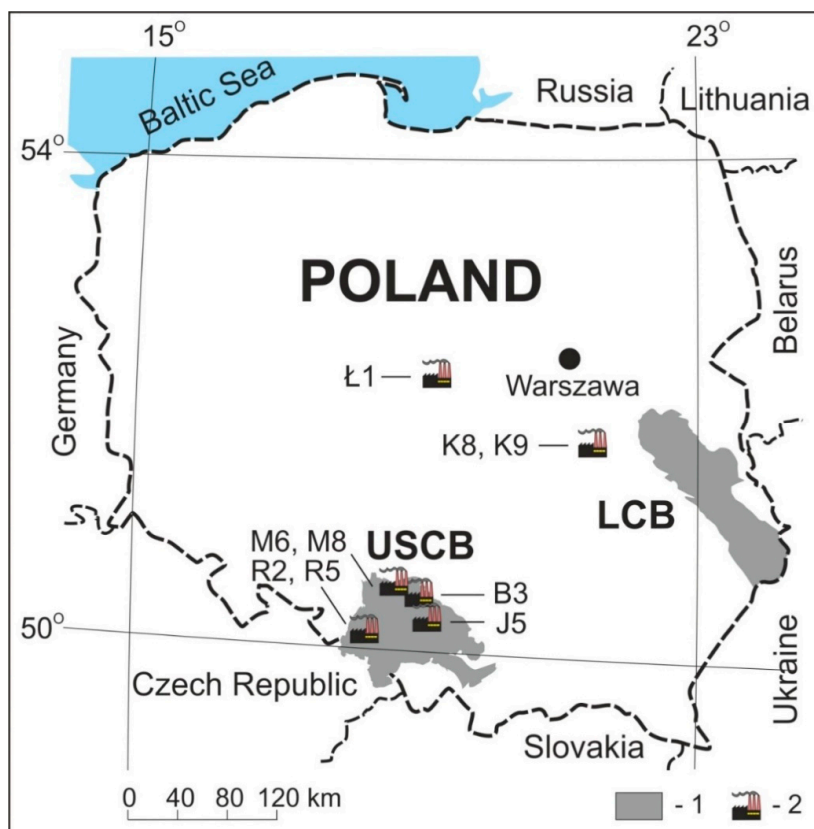


Figure 1. Location of studies area and sampling point: (1) basin areas; (2) power stations that burn coal from LCB (samples symbol: K9, Ł1) and from the USCBC (B3, J5, M6, M8, R2, R5; see Supplementary Materials Table S1).

Air-dried samples of coal and slag feeds were ground into grains with a diameter < 0.2 mm. The fly ash samples were separated by using 5 sieves, into 5 grain classes, i.e., > 0.5 mm, 0.5–0.2 mm, 0.2–0.05 mm, and < 0.05 mm. Due to the visible high iron content, the slag samples were separated by means of a manual magnetic separator into a magnetic and non-magnetic fraction (see Supplementary Materials Table S4).

Ash yield in samples of feed coals, fly ash, and slag was determined in accordance with PN-ISO 1171: 2002 [50]. The results of the determinations are given in Table 1 (see Supplementary Materials Table S3). In the ash samples obtained, the following were determined:

- (1) EE content (Ag, As, Bi, Cd, Co, Cr, Cu, Mn, Mo, Ni, Pb, Sb, Sn, V, W, and Zn) and Fe content was determined by inductively coupled plasma atomic emission spectroscopy (0.25 g of the sample was heated with HNO_3 , HClO_4 , and HF to fuming and brought to dryness. The residue was dissolved in HCl). The analysis was performed by using Spectro Ciros Vision with autosampler SPECTRO AS500, and the analysis conditions specified by Bureau Veritas Canada [51] were retained. The results of this analysis (see Supplementary Materials Table S5) were converted into the content of elements in raw samples Table 2. (see Supplementary Materials Table S6).
- (2) Content of elements in micro-areas of grains of feed coal (made on the cross-section), as well as fly ash and slag (made on whole particles, sprayed on the surface of the film, and made on the cross-section) was determined by the method of scanning electron microscope, using SU-3500 Hitachi model with energy dispersive X-ray UltraDry EDS Detector ThermoFisher Scientific,

and maintaining the standard conditions for performing analyses (acc. Voltage = 15.0 kV, bse-comp = 30 Pa, image resolution = 1024 by 768, image pixel size = 0.04 μm –0.27 μm , magnification = 90–5000). The maximum content of elements in the feed coal, fly ash, and slag is presented in Table 3 (see Supplementary Materials Table S7), and examples of interesting analyses are shown in Figure 2.

Using the Pearson's Chi-square test, the Kolmogorov–Smirnov test, and the Shapiro–Wilk test (with a significance level of $p = 0.05$), the hypothesis regarding the normal distribution of the results of the measurements was tested. Then, the following was calculated:

- (1) Average EE content in the studied feed coals, which were compared with the average EE content in raw bituminous coal from the LCB and the USCB (determined by various authors) and hard-coal Clarke values (see Supplementary Materials Table S6);
- (2) Values of the Pearson correlation coefficient, r , in order to find the relationship between the petrographic composition of feeds coal and ash yield in coal feeds from the LCB and the USCB, and the EE content in feeds coal. The linear regression determination coefficients R^2 were determined for the sought relationships. Verification of the linear regression model was carried out, using the F-Snedecor test at the confidence level $\alpha = 0.05$, and the significance of the correlation coefficient, r , for the significance level, $p < 0.05$, was verified by using the Student's t -test. In the interpretation of r and p values, it was assumed that $r \geq 0.35$ for $p < 0.05$ indicate the significance of the correlation relationship studied. On the other hand, the values of $r \geq 0.35$ for $p = 0.05$ – 0.20 only allow us to state that the statistical analysis did not prove the significance of the correlation; it is assumed that in the case of a wider range of values of the analyzed parameters or the use of different, more accurate measurement methods, the examined relationships would probably be significant. The results of the interpretation of the correlation coefficient value are given in Table 4 and Figure 3a (see Supplementary Materials Tables S8 and S9).
- (3) Average content of EE in the studied fly ash and slag, which was compared with the average content of trace elements from coal ash from hard-coal deposits in the world (see Table 5 and Supplementary Materials Table S10);
- (4) Enrichment factor, in order to determine elements that have been enriched as a result of combustion of feed coals and which have been depleted in fly ash and slag. This factor is the quotient of the element content in fly ash or slag, relative to the element content in the coal feed (see Table 5; see Supplementary Materials Tables S10–S12);
- (5) Average EE content in fly ash grain grades and slag density fractions (see Figure 3a; see Supplementary Materials Table S13);
- (6) The share of fly ash grain classes and slag grain fractions in the concentration of elements in whole fly ash and whole slag was determined. To this end, the percentage share of each weighted average component in the total weighted average was calculated. The weighted average component is the product of the element content in each class of fly ash grains and in each slag fraction, as well as the percentage mass share of each class and grain fraction in the composition of whole fly ash and in the whole slag. The calculation results are shown in Figure 3b (see Supplementary Materials Table S13).

3. Results and Discussion

3.1. Petrographic and Mineral Composition of Coal

Regarding the random reflectance (R_r) of vitrinite (Table 1), feed coals originating from the LCB and the USCB classify as ortho-bituminous coal (after International Classification of Seam Coals, Final Version [52]). Coal feeds from the LCB contain more vitrinite and less inertinite than coal feeds from the USCB. In the mineral matter of the LCB coal feed, pyrite with marcasite, quartz with feldspar,

and kaolinite are most common, and in the USCB coal feed, there is the most dolomite, quartz with feldspar, and kaolinite.

The average ash yield of feed coal (Table 1) is similar to the ash yield of coal burned in power plants in other countries, for example, in Soma in Turkey (A = 40.0%, [53]), in Jungar in China (A = 33%, [26]), and in Bulgaria (A = 42.7%, [54]).

3.2. Evaluation of the Content and Mode of Occurrence of Elements in Feed Coals

The data in Table 2 show that, in feed coals from the LCB, there are higher contents of Ag, As, Cd, Co, Cr, Cu, Fe, Mn, Mo, Ni, Pb, Sn, V, W, and Zn and lower contents of Bi and Sb than in coal feeds from the USCB. It was observed that the content of Ag, As, Bi, Cd, Co, Mo, Sb, and W in feed coals from the LCB, and the content of Ag, As, Cd, Co, Cu, Mo, Pb, Sb, and Zn in feed coals from the USCB, is lower than in raw coal from the LCB and the USCB. In contrast, the content of Cr, Cu, Fe, Mn, Ni, Pb, Sn, V, and Zn in feed coals from the LCB, and the content of Bi, Cr, Fe, Mn, Ni, Sn, V, and W in feed coals from the USCB is greater than in raw coal. Compared to hard-coal Clarke values, the average content of Ag, Co, Cr, Cu, Mn, Mo, Ni, Pb, Sn, V, W, and Zn in feed coals from the LCB and the USCB and As in feed coals from the LCB is higher. However, the content of Bi, Cd, and Sb in feed coals from the LCB and from the USCB is similar or smaller.

In feed coals from the LCB, the highest point of EE content was recorded in siderite (As, Bi, Co, Cu, Fe, Mn, Pb, Sb, Sn, and V), pyrite (Ag, Cd, Mo, Ni, and Zn), and sporadically in clay minerals (Cr, see Table 3 and Supplementary Materials Table S7). However, in the USCB feed coals, the highest content of elements is found in siderite (Bi, Cu, Mn, Sb, and V), magnetite (Co, Fe, and Ni), fusinite (Ag, As, and W), clay minerals (Cr and Sn), vitrinite (Zn), liptinite (Cd), ankerite (Pb), and pyrite (Mo). These minerals are quite often a source of EE in feed coals burned in various power plants (e.g., [20,55]). Admixtures of elements not included in the chemical composition of macerals and minerals most often come from inclusions of native minerals (e.g., chalcopyrite, galena, and sphalerite), inclusions enriched in EE (e.g., siderite enriched in Mn, ankerite enriched in Pb [56–61]), and organometallic bonds in low-rank coal [62–64].

Table 1. Petrographic characteristics, vitrinite reflectance, and ash yield of feed coals from the LCB and USCB, and fraction yields of the fly ash and slag.

Characteristics	LCB		USCB	
	Range	Arithmetic Average	Range	Arithmetic Average
Vitrinite (vol. %)	66.1–72.0	69.4	46.3–68.1	58.9
Liptinite (vol. %)	2.3–6.9	4.3	2.1–6.9	5.0
Inertinite (vol. %)	10.1–12.0	11.0	11.1–31.6	21.3
Mineral matter (vol. %)	14.8–16.1	15.3	6.2–24.8	14.8
Sulfide minerals (wt %)	6.2–7.9	6.9 (py) *	0.2–3.6	1.4 (py) *
Magnetite+hematite (wt %)	< 0.1–0.3	0.1 (m) *	0.1–0.4	0.2 (m) *
Quartz+feldspar (wt %)	3.3–4.2	3.8 (q) *	0.5–8.9	4.2 (q) *
Clay minerals (wt %)	2.2–3.2	2.8 (ka) *	0.3–12.8	3.6 (ka) *
Carbonate minerals (wt %)	0.7–2.8	1.5 (sd) *	0.5–10.9	5.4 (do) *
Sulphate minerals (wt %)	< 0.1–0.5	0.2 (gy) *	<0.1–0.1	< 0.1 (gy) *
Phosphate minerals (wt %)	< 0.1–0.1	< 0.1 (a) *	<0.1–0.2	< 0.1 (a) *
Vitrinite reflectance (%)	0.67–0.71	0.69	0.67–0.92	0.74
Ash yield (wt %)	25.53–41.03	33.13	11.38–43.92	22.83
Fraction yields (wt%)				
> 0.5 mm	0.15–6.49	3.29	< 0.01–0.65	0.33
0.5–0.2 mm	20.29–21.18	20.67	1.90–15.69	5.99
0.2–0.05 mm	41.52–44.49	43.01	16.51–65.80	38.48
< 0.05 mm	27.84–37.93	33.04	27.37–81.18	55.20
Slag, magnetic	11.47–13.73	12.60	5.67–32.47	10.61
Slag, nonmagnetic	86.27–88.53	87.40	67.53–94.33	89.39

* Main minerals identified by X-ray (py—pyrite+marcasite, m—magnetite, q—quartz, ka—kaolinite, sd—siderite, do—dolomite, gy—gypsum, and a—apatite).

Table 2. Average contents of elements in raw coal and in feed coals from the LCB and USCB compared to hard-coal Clarke values (HCCV).

Element *	HCCV (after Ketris and Yudo Vich [65])	LCB			USCB		
		Raw	Feed Coal		Raw	Feed Coal	
		Coal **	Range	Aa ***	Coal **	Range	Aa ***
Ag (ppm)	0.100 ± 0.016	0.57 ⁶	0.1–0.4	0.3	1–2 ³	0.1–0.4	0.2
As (ppm)	9.0 ± 0.7	47 ¹	18.5–25.2	21.5	9 ¹	1.1–17.0	5.8
Bi (ppm)	1.1 ± 0.1	0.6 ⁷	< 0.1–0.1	< 0.1	nd	< 0.1–1.4	0.4
Cd (ppm)	0.20 ± 0.04	2.3 ⁴	0.1–0.6	0.3	1.2 ²	< 0.1–0.3	0.1
Co (ppm)	6.0 ± 0.2	43.5 ²	15.5–17.4	18.6	15.0 ⁸	4.5–18.3	8.4
Cr (ppm)	17 ± 1	17.5 ²	165.6–233.2	187.6	37.0 ⁸	30.6–179.8	94.1
Cu (ppm)	16 ± 1	30.7 ²	23.1–69.9	51.7	42.0 ⁸	17.3–51.5	27.3
Fe (wt %)	Nd	nd	3.81–6.99	4.89	nd	0.72–5.19	1.87
Mn (ppm)	71 ± 5	70.2 ²	556.2–998.7	745.1	192.0 ⁸	126.2–778.6	285.7
Mo (ppm)	2.1 ± 0.1	42.4 ²	4.4–5.3	4.8	44.2 ²	0.7–3.9	2.2
Ni (ppm)	17 ± 1	56.5 ²	99.2–155.6	123.4	31.0 ⁸	28.2–117.1	58.1
Pb (ppm)	9.0 ± 0.7	27 ⁵	35.3–45.0	39.4	35.0 ⁸	12.2–36.5	24.4
Sb (ppm)	1.00 ± 0.09	1.5 ¹	< 0.1–0.1	< 0.1	1.1 ¹	< 0.1–2.8	0.7
Sn (ppm)	1.4 ± 0.1	0.5 ⁶	5.2–10.5	7.3	nd	1.2–8.6	3.0
V (ppm)	28 ± 1	91.0 ²	99.8–146.3	127.7	42.0 ⁸	21.6–130.0	51.2
W (ppm)	0.99 ± 0.11	3.5 ⁶	1.0–2.4	1.9	nd	< 0.1–4.4	1.2
Zn (ppm)	28 ± 2	33.2 ²	58.0–93.5	72.0	94.0 ⁸	29.6–86.3	57.1

* Detection limit of elements in feed-coal ash: Ag = 0.5 ppm; As, Bi, Mn, Pb, and Sb = 5 ppm; Cd = 0.4 ppm; Co, Cr, Cu, Mo, Ni, Sn, V, and Zn = 2 ppm; Fe = 0.01 wt%; W = 4 ppm. ** Average value after 1—Bojakowska and Pasieczna [66], 2—Cebulak [67] 3—Hanak and Kokowska-Pawłowska [68], 4—Marczak and Parzentny [69], 5—Marczak and Parzentny [70], 6—Parzentny [71], 7—Parzentny and Róg [72], and 8—Ptak and Rózkowska [73]; nd—no data
*** Arithmetic average.

Based on the suggested interpretation results of the calculated values of the Pearson correlation coefficient (see Table 4; see Supplementary Materials Tables S8 and S9), it was assumed that As, Cd, Co, Cr, Cu, Fe, Mn, Mo, Ni, Pb, Sn, and Zn are probably bound in LCB feed coal to carbonate minerals; Ag, As, Sn, V, and W with vitrinite or liptinite; Sn with sulphate minerals; and As and Sn with feed coal ash (i.e., with organic and generally mineral matter). On the other hand, in feed coals from the USCB, Ag, As, Mo, and Ni are probably bound to vitrinite; Fe, Pb, and Zn to pyrite and marcasite; Zn only to carbonates; Sb only to sulphate minerals; and Ag, Co, Cr, Cu, Fe, Mn, Mo, Ni, Sn, V, and W to feed-coal ash (i.e., with matter generally organic and generally mineral). The correlation between the content of quartz and feldspars and the content of EE in feed coals was not interpreted, due to the insignificant content of elements in these minerals. There were no grounds to determine the mode of binding Bi and Sb in coal feeds from the LCB (content below detection limit) and Bi and Cd in feed coals from the USCB (no correlation). Bismuth in raw bituminous coal from world deposits [5,14] and from the USCB and the LCB [72,74,75] is associated with organic matter in general, while Cd is associated with sulfide minerals. The mode of occurrence of EE in feed coals is probably individual to each feed coal and can differ from the mode of binding in raw coal. For example, the data in Table 4 suggest binding Ag in feed coals from the LCB probably to vitrinite, and Zn to carbonate minerals. In contrast, previous studies on raw coal from the LCB indicate a binding of Ag to a comparable degree to clay minerals and vitrinite [71], and Zn to both organic and mineral raw coal [76]. The binding mode of trace elements in coal is probably differentiated in raw coal within the basin and individual lithostratigraphical series [5,77–79], and even in individual parts of a single coal seam [80,81]. The content and mode of binding of EE in coal feeds is probably different before and different after the removal of mineral matter from the coal feeds at the mineral enrichment plant [30,31,82–86]. It seems justified to monitor the content and binding mode of EE in coal before its purchase and before the coal is intended for combustion.

Table 3. Maximum content (wt%) of element in feed coals from the LCB and USCB and in the fly ash and slag obtained by the SEM/EDS method.

Element *	Feed Coal				Fly Ash				Slag			
	LCB		USCB		LCB		USCB		LCB		USCB	
	Content	Compound	Content	Compound	Content	Compound	Content	Compound	Content	Compound	Content	Compound
Ag	0.10	pyrite	0.12	fusinite	0.02	Al-Si sphere	0.32	crassisphere	0.12	Al-Si grain	0.28	Al-Si sphere
As	0.25	siderite	0.41	fusinite	0.31	magnetite skelet. **	0.27	Al-Si sphere	0.24	Al-Si grain	0.30	Al-Si grain
Bi	0.30	siderite	0.47	siderite	0.13	Al-Si sphere	0.55	Al-Si sphere	< 0.01	no data	< 0.01	no data
Cd	0.02	pyrite	0.26	liptinite	< 0.01	no data	0.13	crassisphere	0.29	magnetite skelet. **	0.21	Al-Si sphere
Co	0.12	siderite	0.20	magnetite	0.14	Al-Si sphere	0.14	Al-Si sphere	0.10	Al-Si sphere	0.67	Al-Si grain
Cr	0.02	clay	0.03	clay	0.21	magnetite skelet.	2.00	magnetite dendr. **	0.17	magnetite skelet. **	0.16	magnetite skelet. **
Cu	0.16	siderite	0.43	siderite	0.18	magnetite dendr. **	1.29	magnetite skelet. **	0.07	Al-Si grain	0.22	magnetite dendr. **
Fe	46.88	siderite	57.85	magnetite	51.58	magnetite skelet. **	56.65	magnetite skelet.*	57.59	magnetite skelet. **	69.51	magnetite skelet. **
Mn	1.45	siderite	2.08	siderite	0.56	magnetite skelet. **	0.87	magnetite skelet. **	0.23	magnetite skelet. **	3.77	Al-Si sphere
Mo	3.21	pyrite	5.92	pyrite	0.38	Al-Si sphere	1.01	magnetite grain**	0.94	magnetite skelet. **	1.84	Al-Si sphere
Ni	0.07	pyrite	6.52	magnetite	0.33	Al-Si sphere	0.88	magnetite skelet. **	0.14	Al-Si grain	0.27	magnetite grain**
Pb	0.08	siderite	1.07	ankerite	0.94	magnetite skelet. **	0.50	Al-Si sphere	0.38	Al-Si grain	1.72	magnetite grain**
Sb	0.21	siderite	0.57	siderite	0.45	magnetite skelet.	0.95	magnetite skelet. **	0.40	magnetite skelet. **	0.36	Al-Si sphere
Sn	0.13	siderite	0.51	clay	0.70	Al-Si sphere	0.61	magnetite grain	0.27	magnetite skelet. **	1.34	Al-Si sphere
V	0.04	siderite	0.37	siderite	0.18	Al-Si sphere	0.38	Al-Si sphere	0.12	magnetite skelet. **	0.31	Al-Si grain
W	< 0.01	no data	0.83	fusinite	0.68	Al-Si sphere	2.47	Al-Si sphere	0.53	magnetite skelet. **	1.42	crassisphere
Zn	0.03	pyrite	0.50	vitrite	0.19	magnetite skelet. **	1.18	crassisphere	0.19	magnetite skelet. **	0.80	Al-Si grain

* Detection limit of the elements = 0.01 wt %. ** The magnetite (skeletal, dendrite) form grew on aluminum-silicate (Al-Si) microsphere or cenosphere.

Table 4. Supposed modes of occurrence of elements in the feed coal.

Coal Basin	Element	Component of the Feed Coal
Lublin	Ag	Vitrinite (Vt)
	As	Liptinite (L), carbonate minerals (Cb)
	Bi	No data
	Cd	Carbonate minerals (Cb)
	Co	Carbonate minerals (Cb)
	Cr	Carbonate minerals (Cb)
	Cu	Carbonate minerals (Cb)
	Fe	Carbonate minerals (Cb)
	Mn	Carbonate minerals (Cb)
	Mo	Carbonate minerals (Cb)
	Ni	Carbonate minerals (Cb)
	Pb	Carbonate minerals (Cb)
	Sb	No data
	Sn	Liptinite (L), carbonate minerals (Cb), sulphates (SF)
	V	Vitrinite (Vt)
	W	Vitrinite (Vt)
	Zn	Carbonate minerals (Cb)
Upper Silesian	Ag	Vitrinite (Vt), coal ash (A)
	As	Vitrinite (Vt), pyrite+marcasite (Py)
	Bi	No data
	Cd	No data
	Co	Vitrinite (Vt), coal ash (A)
	Cr	Coal ash (A)
	Cu	Coal ash (A), quartz+felspar (QF)
	Fe	Pyrite+marcasite (Py), coal ash (A)
	Mn	Coal ash (A), quartz+felspar (QF)
	Mo	Vitrinite (Vt), coal ash (A)
	Ni	Vitrinite (Vt), coal ash (A)
	Pb	Pyrite+marcasite (Py)
	Sb	Sulphate minerals (Sf)
	Sn	Coal ash (A), quartz+felspar (QF)
V	Coal ash (A)	
W	Coal ash (A)	
Zn	Pyrite+marcasite (Py), carbonate minerals (Cb)	

3.3. Distribution of Elements in Fly Ash and Slag

Phase-minerals of high ash and slag with the highest EE content were identified, using a scanning microscope (see Table 3, Figure 2, and Supplementary Materials Table S7). In fly ash originating from combustion of feed coals from the LCB, the highest content of elements was found in Al-Si microspheres (Ag, Bi, Co, Mo, Ni, Sn, V, and W) and in magnetite with skeletal or dendritic structure crystallized on the Al-Si surface of microspheres or cenospheres (As, Cr, Cu, Fe, Mn, Pb, Sb, and Zn). On the other hand, in fly ash from the USCB feed coals, the highest content of elements was determined in magnetite with dendritic, skeletal, or granular structure crystallized on the surface of Al-Si microspheres or cenospheres (Cr, Cu, Fe, Mn, Mo, Ni, Sb, and Sn) and in Al-Si microspheres (As, Bi, Co, Pb, V, and W), and less often in crassispheres (Ag, Cd, and Zn). In the slag from the combustion of coal feeds from the LCB, the highest content of elements was found in magnetite with skeletal structure crystallized on the surface of Al-Si microspheres or cenospheres (Cd, Cr, Fe, Mn, Mo, Sb, Sn, V, W, and Zn) and in Al-Si microspheres or grains (Ag, As, Co, Cu, Ni, and Pb); in turn, in the slag from the USCB feed coals, the highest content of elements was determined in Al-Si microspheres or grains (Ag, As, Cd, Co, Mn, Mo, Sb, Sn, V, and Zn) of magnetite with a skeletal, dendritic, or granular crystallized on the surface of Al-Si microspheres or cenospheres (Cr, Cu, Fe, Ni, and Pb), and less often in crassispheres (W). The morphological forms of fly ash and slag phase-minerals listed above are the most common among combustion waste resulting from the combustion of coal feeds in Poland and in the world (e.g., [41,54,87,88]). These phases are often characterized by high EE content, which has already been demonstrated by studies of phase-minerals group concentrates and concentrates of morphological forms of combustion residues [26,89–91].

The data in Table 5 show that the content of most of the EEs analyzed in the tested fly ash and slag are comparable or lower than the content of EE in hard-coal ash from world deposits. Only the content

of Ni and V in fly ash and coal slag from the LCB, and the content of Mn, Pb, V, and Zn in fly ash and the Mn content in coal slag from the USCB are higher than the content of these elements in world coal ash. Although the geochemical features of hard-coal ash, fly ash, and slag differ, the comparison suggested above indicates that solid coal-burning products in Poland are probably less dangerous to the environment than from power plants in other countries. In addition, they are of little use to EE recovery.

Due to the value of the enrichment factor (EF) (see Table 5 and Supplementary Materials Table S12), elements found in fly ash and slag are divided into seven groups:

1. Highly enriched elements ($EF \geq 2.0$) in fly ash (from the LCB: Ag, Co, Cu, V, and W; and from the USCB: Ag, As, Bi, Cd, Co, Cu, Fe, Mn, Mo, Pb, Sb, V, W, and Zn);
2. Highly enriched elements in slag (the LCB: V; the USCB: Ag, Bi, Cd, Co, Cu, Fe, Mn, V, and Zn);
3. Weakly enriched elements ($EF = 1.0\text{--}2.0$) in fly ash (LCB: As, Ni, Pb, and Zn; USCB: Cr, Ni, and Sn);
4. Weakly enriched elements in slag (LCB: Co and Cu; USCB: Cr, Ni, and Pb);
5. Depleted elements ($EF < 1.0$) in fly ash (the LCB: Cd, Cr, Fe, Mn, Mo, and Sn; the USCB: none);
6. Elements depleted in slag (the LCB: Ag, As, Cr, Fe, Mn, Mo, Ni, Pb, Sn, and Zn; the USCB: As, Mo, Sb, Sn, and W);
7. Elements not found in fly ash (only from the LCB: Bi and Sb) and in slag (only from the LCB: Bi, Cd, Sb, and W).

In general, all the elements were enriched more in whole fly ash than in whole slag. Maximum (10-fold) enrichment was observed for Cd and Bi in fly ash from the USCB feed coal. However, the maximum (16-fold) point enrichment of Ag was recorded in Al-Si cenosphere in fly ash, resulting from the combustion of coal from USCB (Figure 2). The above observations confirm the previously noted regularity, consisting in more intensive condensation and enrichment of the majority of EE on fly ash particles than on slag particles and bottom ash [8,14,20,26,42]. According to Wang et al. [28], the described tendency results from a specifically developed surface, greater surface activity, and the ability to adsorb fine, rather than coarse, fly ash and slag particles.

Based on the data presented in Figure 3a (see Supplementary Materials Table S13), it was observed that the highest content of Cd, Co, Cu, Mn, Ni, Pb, Sn, V, W, and Zn in fly ash resulting from feed coals from the LCB and the USCB occurs in fly ash particles < 0.05 mm. The same is true for the content of As, Cr, Fe, and Mo in fly ash from feed coals from the LCB and Sb from feed coals from the USCB. This group of particles, with a large share in the composition of whole fly ash (Table 1), also has the greatest impact on the average content of these elements in whole fly ash (see Figure 3b and Supplementary Materials Table S13). The highest content of remaining elements in fly ash from the LCB (Ag) and the USCB (Ag, As, Bi, Cr, Fe, and Mo) was recorded in the least numerous (Table 1) group of particles, i.e., with a size > 0.5 mm (Figure 3a); in turn, particles with a size of 0.05 mm–0.2 mm or < 0.05 mm have the greatest impact on the content of these elements in whole fly ash (Figure 3b). The presence of Bi and Sb was not found in fly ash particles from combustion of feed coals from the LCB. The highest content of most elements in the slag resulting from the combustion of feed coals from the LCB (Co, Fe, Mn, Ni, and Zn) and the USCB (Ag, As, Bi, Cd, Co, Cr, Fe, Mn, Ni, Pb, Sn, V, W, and Zn) was found in the magnetic fraction of slag (Figure 3a). However, the largest content and, therefore, impact on the content of elements in the whole slag has the non-magnetic fraction of slag (Figure 3b). This is due to greater yields of the non-magnetic fraction in the whole slag composition than the magnetic fraction (Table 1). The magnetic fraction has the highest content and also the largest influence on the content of some elements in the whole slag from the LCB feed coals (Ag, As, and Mo) and from the USCB (Mo and Sb) (Figure 3). This is due to the absence or low content of elements in the non-magnetic slag fraction. However, the largest content and the largest impact on the content of Cr, Cu, Pb, Sn, and V in the whole slag from the LCB coals has the non-magnetic fraction.

Table 5. Enrichment factor (EF) of elements in fly ash and slag relative to the content of elements in coal feeds from the LCB and the USCB, as well as allowable concentrations of elements in soil determined (in accordance with Polish Journal of Laws 2016 item 1395, 2016; [92]) for group I soils (PCS) and the content of elements in coal ash from world deposits.

Element	PCS (ppm)	LCB								USCB				
		World *		Fly Ash		Slag				Fly Ash		Slag		
		Coal Ash	Range	Aa **	EF	Range	Aa **	EF	Range	Aa **	EF	Range	Aa **	EF
Ag	no data	0.63 ± 0.01	0.8–0.9	0.8	2.7	0.1	0.1	0.3	< 0.1–1.8	0.7	3.5	< 0.1–2.1	0.5	2.5
As	25	46 ± 5	22.5–25.2	23.9	1.1	0.4–0.6	0.5	0.02	3.5–29.0	17.0	2.9	< 0.1–4.8	1.9	0.3
Bi	no data	7.5 ± 0.4	< 0.1	< 0.1	no data	< 0.1	< 0.1	no data	< 0.1–11.1	3.5	8.8	< 0.1–5.9	1.0	2.5
Cd	2.0	1.20 ± 0.30	0.1–0.2	0.2	0.7	< 0.1	< 0.1	no data	< 0.1–2.6	1.0	10.0	< 0.1–1.9	0.8	8.0
Co	50	37 ± 2	36.4–40.6	38.6	2.1	31.6–35.9	33.6	1.8	17.9–39.4	34.0	4.0	18.3–28.9	23.2	2.8
Cr	200	120 ± 5	131.8–143.6	138.4	0.7	117.8–127.1	123.4	0.7	67.7–133.3	110.0	1.2	81.8–124.3	97.1	1.0
Cu	200	110 ± 5	99.3–104.0	103.7	2.1	76.1–81.1	79.1	1.5	91.5–196.6	126.3	4.6	59.9–106.1	87.5	3.2
Fe	no data	no data	4.07–4.23	4.2	0.9	4.59–4.89	4.8	1.0	4.62–9.17	7.0	3.7	3.02–8.13	5.5	2.9
Mn	no data	430 ± 30	285.3–306.8	294.4	0.4	332.3–355.5	342.5	0.5	579.8–1452.0	962.3	3.4	531.2–1173.6	827.7	2.9
Mo	50	14 ± 1	3.6–4.4	4.1	0.9	0.3–0.5	0.4	0.1	0.9–8.0	5.0	2.3	< 0.1–3.2	1.4	0.6
Ni	150	100 ± 5	133.1–144.9	135.9	1.1	115.4–124.3	120.2	1.0	58.2–124.5	99.0	1.7	52.6–95.0	69.2	1.2
Pb	200	55 ± 6	52.2–57.0	54.3	1.4	19.6–24.2	22.1	0.6	40.3–221.2	104.1	4.3	22.6–66.5	39.2	1.6
Sb	no data	7.5 ± 0.6	< 0.1	< 0.1	no data	< 0.1	< 0.1	no data	< 0.1–7.9	4.2	6.0	< 0.1	0.4	0.6
Sn	20	8.0 ± 0.4	4.4–5.5	4.7	0.6	2.4–3.4	2.9	0.4	0.1–8.2	4.8	1.6	< 0.5–3.1	1.2	0.4
V	no data	170 ± 10	290.0–308.1	297.9	2.3	247.4–273.0	261.3	2.05	126.8–249.0	197.9	3.9	125.2–190.1	160.8	3.1
W	no data	7.8 ± 0.6	5.4–6.0	5.7	3.0	< 0.1	< 0.1	no data	0.5–6.0	3.2	2.7	< 0.1–4.9	0.7	0.6
Zn	500	170 ± 10	84.4–94.7	87.1	1.2	33.7–39.7	37.3	0.5	139.5–440.3	231.0	4.0	67.6–214.3	121.9	2.1

* Content (ppm) after Ketris and Yudovich [55]; ** arithmetic average.

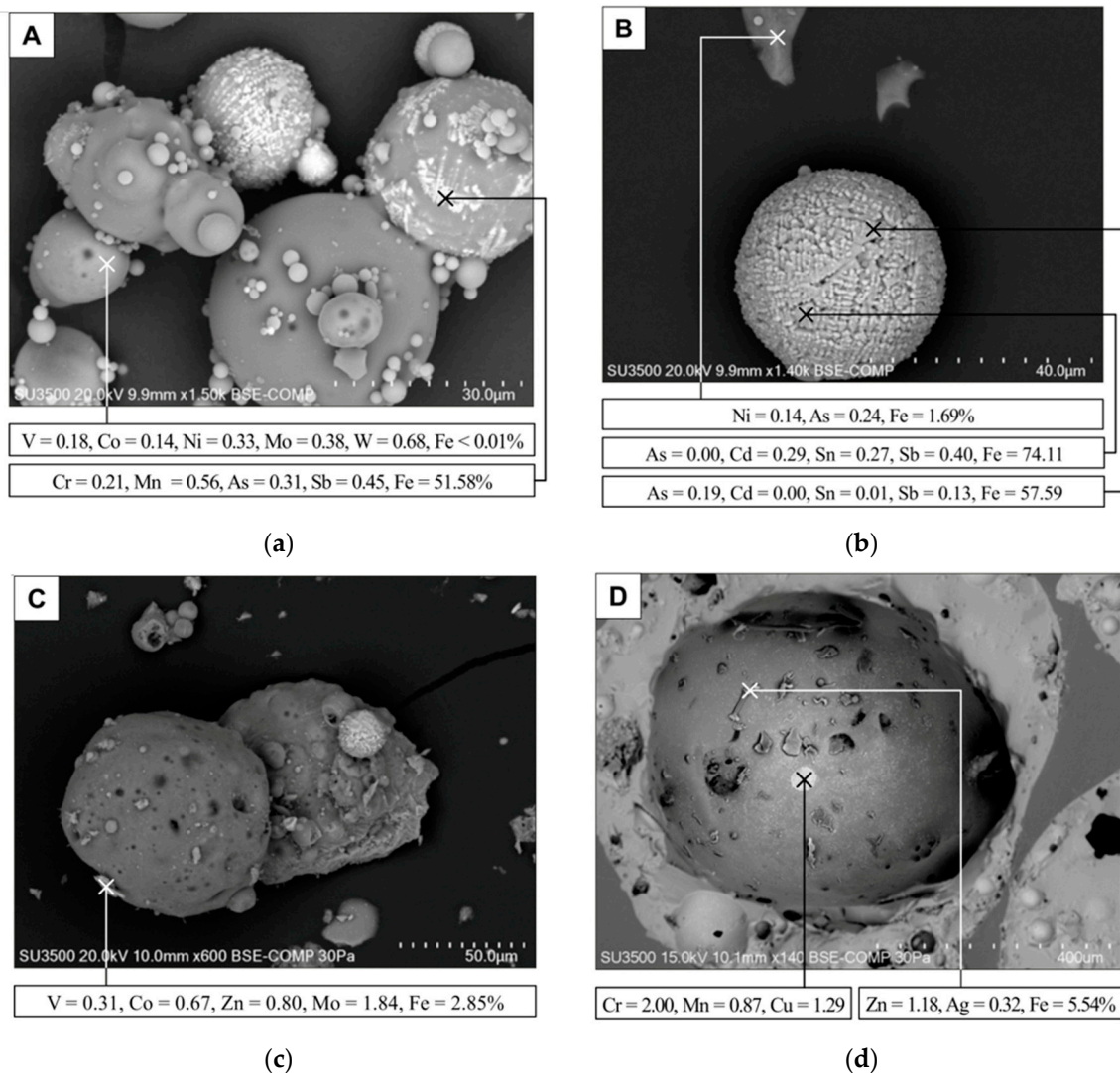


Figure 2. Sample results of the SEM/EDS analysis of elements content (% wt) in (a) Al-Si microspheres with magnetite skeletal and dendrites in fly ash (sample K9, feed coal from the LCB); (b) Al-Si grain and Al-Si microsphere with magnetite skeletal in fly ash (sample K9, feed coal from the LCB); (c) isolated magnetite crystal on Al-Si grains from slag (sample J5, feed coal from the USCB); and (d) Al-Si cenosphere in fly ash (sample M6, feed coal from the USCB).

This is due to both the relatively low content of these elements in the magnetic fraction (Figure 3a) and the small yields of the magnetic fraction in the composition of the whole slag (Table 1). The presence of Bi, Cd, Sb, and W was not found in the slag from combustion of feed coals from the LCB (see Supplementary Materials Table S13). It was also observed that the EE content in the fly ash grain classes, mostly these enriched with elements, is generally higher than in the most enriched group of slag particles (Figure 3a). Only the content of Fe and Mn in magnetic slag particles from the LCB feed coals and the content of Mn in the magnetic slag particles from the combustion of coals from the USCB is higher than in the grades of fly ash particles.

The accumulation of EE in fly ash and slag is generally negatively assessed, as these elements can prevent the industrial use of fly ash and slag and contribute to soil and groundwater contamination. Fly ash and less often slag are currently widely used as building material, as fillers in asphalt, mineral fertilizers, concrete pavements, soil, roads, embankments, and mine voids, as well as for the production of zeolites and geopolymers, etc. Fly ash is most often used as a high-performance replacement for the production of Portland cement. (e.g., [2,93,94]). Due to the lack of requirements regarding the

acceptable EE content in fly ash and slag before it is used in construction, it is difficult to assess whether the EE content determined in the tested samples can be considered dangerous for the environment. However, following the regulation of the Polish Ministry of the Environment regarding criteria for the classification of extractive waste [95] based on the Regulation of the European Union [96], it was assumed that solid waste from the combustion process of the studied coal feeds can be considered inert if the EE content in this waste does not exceed the soil quality standards specified for group I soils. In this regulation, As, Cd, Co, Cr, Cu, Mo, Ni, Pb, Sn, and Zn are classified as potentially hazardous substances for which limit values have been set. Group I soils refer to agricultural soils, forests and urbanized areas (excluding industrial areas), barren and fossil lands, and road transport infrastructure [92]. Based on the data contained in Table 5, it was determined that the average content of As, Cd, Co, Cr, Cu, Mo, Ni, Pb, Sn, and Zn in fly ash and slag from feed coals from the LCB and the USCB did not exceed the allowable value for soils from group I. Therefore, solid combustion waste tested can be considered as inert waste. Nevertheless, considering fly ash divided into grain size classes and slag divided into fractions (Supplementary Materials Table S10), it was observed that few fly ash samples with particle size > 0.5 mm and < 0.05 mm from the LCB feed coals can be classified as hazardous waste due to the high content of As, Co, and Ni. The same is true for feed coals from the USCB due to the high content of As, Cd, Co, Cr, Cu, Ni, and Pb. It seems reasonable to monitor the EE content in the smallest groups of fly ash particles generated in power plants. When accumulations of tested fly ash with dangerously high EE content are exposed to rainwater, infiltrating, and standing and/or flowing water, they can release toxic effluents to the environment. Out-flowing concentrations expressed in absolute terms certainly differ; however, leaching appears to be relatively the same and takes place according to the same standards [2,97]. The mobility of trace elements in water is highly dependent on pH. The calcium to sulfur ratio determines the pH of the ash with water system and plays a dominant role in the leaching of most EE from fly ash. While alkalinity contributes to the weakening of the ability to leach large amounts of EE, it also increases their mobility of several types of oxyanions, i.e., As, Cr, Mo, Sb, V, and W. A large part of the elements discussed in this paper (Cd, Co, Cu, Fe, Mn, Ni, Pb, Sn, and Zn) is characterized by the fact that their minimum solubility is reached at pH 7–10. These elements can be considered [2,6] hazardous in alkaline fly ash in natural environment conditions (i.e., slightly acidic to alkaline). The opposite is true for acid fly ash, as the mobility of EE in aqueous solutions increases with decreasing pH. Summing up the above speculations, it can be assumed that, under the influence of a slightly acidic environment, from the particles of tested fly ashes, these EEs may undergo slow leaching. There is a concern that even small concentrations of EE in aqueous leachate can penetrate into groundwater, and in the upper soil layers, they become bioavailable and reach the food chain of humans and animals [98,99].

Analyzing the data given in Figure 3 (see Supplementary Materials Table S13), a correlation was observed between the mode of binding of elements in the tested coals and the distribution of elements in fly ash and slag.

- A. When coal is burned, which contains elements probably associated partly or exclusively with vitrinite and/or liptinite and partly or only with organic matter (as a whole), then we get the following:
- The highest content of Ag (feed coal from the LCB and the USCB) and As, Bi, Cr, Fe, and Mo (the USCB) are found in fly ash particles > 0.5 mm in size;
 - Co, Cr, Cu, Mn, Mo, and Ni enrichment index in fly ash (feed coal from the USCB) is higher than when these elements are bound in feed coals (from the LCB) only with carbonate minerals;
 - Elements characterized by a higher melting point than the average combustion temperature of feed coals are in fly ash (formed from the LCB coals: V and W; formed from the USCB coals: Co, Cr, Mo, Ni, V, and W) and in slag (the LCB: V and W; the USCB: Co, Ni and V, respectively) strongly or poorly enriched.

- B. When coal is burned, in which the elements are probably associated with carbonate minerals (coal feeds from the LCB: Cd, Co, Cr, Cu, Fe, Mn, Mo, Ni, Pb, and Zn) and/or with sulphate minerals (the USCB: Sb) and/or sulfide (the USCB: Cd, Pb, and Zn), then fly ash particles < 0.05 mm have the highest content of combustion residues, and these particles have the greatest impact on the content of elements in whole fly ash.
- C. When coal feeds are burned, in which the elements are probably associated with sulfide minerals (the USCB feed coals: Cd, Fe, Pb, and Zn), then the element enrichment index in fly ash is greater than when the elements are in feed coals (from LCB) are bound to carbonate minerals.

The presented relationships show that the total or partial binding of elements to organic matter increases the volatility of elements with both lower and higher melting points than the combustion temperature of coal feed in PS (1280 °C). It was also observed that total or partial binding of elements in feed coals with sulfides (Pb and Zn) increases the enrichment of elements on fly ash and slag particles. Although these relationships are consistent with previously noted results of studies by other authors [8,14,15,20], it is worth verifying these relationships for coal from various basins and for combustion waste from various power plants, so that this relationship has the rank of basic regularity.

Based on the data contained in Figure 3 (see also Supplementary Materials Table S13), it was observed that some elements (Ag, As, Bi, Cr, Fe, and Mo) that easily escape from organic matter during the combustion of feed coals condense more intensively on large (>0.5 mm) than on fine (<0.05 mm) fly ash particles. On the other hand, the elements which evaporate from sulfide, sulphate, and/or carbonate minerals condense most intensively on fine fly ash particles < 0.05 mm in size, and this group of particles has the greatest impact on the average content of elements in whole fly ash. A smaller mass of some EE (Co, Cr, Cu, Mn, Mo, and Ni) which evaporate and then condense on the fly ash particles of was observed when in feed coals these elements are bound to carbonate minerals than when they are bound to organic matter. This is due to the lower temperature of oxidation, combustion and release of elements related to the organic matter of subbituminous and bituminous coal (200–700 °C, according to Vassileva and Vassilev [54]) and a larger volume of organic matter in the studied coal feeds (Table 1), than carbonate minerals (300–900 °C). Smaller condensation of some elements (Cd, Fe, Pb, and Zn) was found on fly ash particles when in coal feed they are bound to carbonates than when they are bound to sulfide minerals. This is due to the lower oxidation temperature of pyrite and marcasite (100–500 °C) than carbonate minerals (300–900 °C). It is assumed that the discussed relationships may be useful for predicting the content and distribution of elements in combustion residues. It is worth remembering, however, that the behavior of EE in the combustion process depends on both the fuel characteristics and operating conditions. Even a moderate change in coal composition and/or combustion conditions can lead to fundamentally different results and researchers may reach different conclusions. There is therefore a need to monitor the distribution of elements both in coal feeds and in solid products of its combustion.

It can be presumed that the combustion of LCB and USCB coal with a high content of EE mainly or exclusively with organic matter may contribute to a significant (even 10-fold) increase in their content in the composition of flue gas from PS furnaces (see Table 5 and Supplementary Materials Table S12). Organic binding of elements in coal feeds can be assessed as unfavorable for obtaining clean, EE-free energy fuel. Removal of elements from macerals and submicroscopic minerals of these elements from coal by means of gravity separation and flotation is considered inefficient, because the content of EE in purified coal is probably still much higher than the average content of EE in global hard coals [30,31,82,83,86]. It is currently believed that the rate of removal of thiophilic and siderophilic elements (Co, Ni, Cu, Zn, As, Cd, and Pb) by gradual flotation is higher than that of lithophilic elements (Sc, Rb, and Ba and Tl) [32]. Multistage purification helps separate toxic elements from purified coals. It is anticipated that the elements Ag, As, Sn, V, and W related to the organic matter of the tested LCB coals, and the elements Ag, As, Co, Mo, and Ni from the USCB, will be difficult to remove. Only chalcophilic elements found in epigenetic sulfides can be removed from coal by using satisfactory gravity and/or flotation [83–85]. The optimal solution, however, will be to avoid

burning coal rich in EE, preceded by monitoring its content in raw coal or feed coals. This success has reportedly been achieved in the USA [100]. Ultrafine ferrospheres and Al-Si particles emitted into the atmosphere from Fe dendritic crystals (Table 3) can also increase the magnetic susceptibility of topsoil layers. For a long time, these frequencies have been identified in the surroundings of power plants [101–106], and with them, the EE content in soil, water, and plants [107–109].

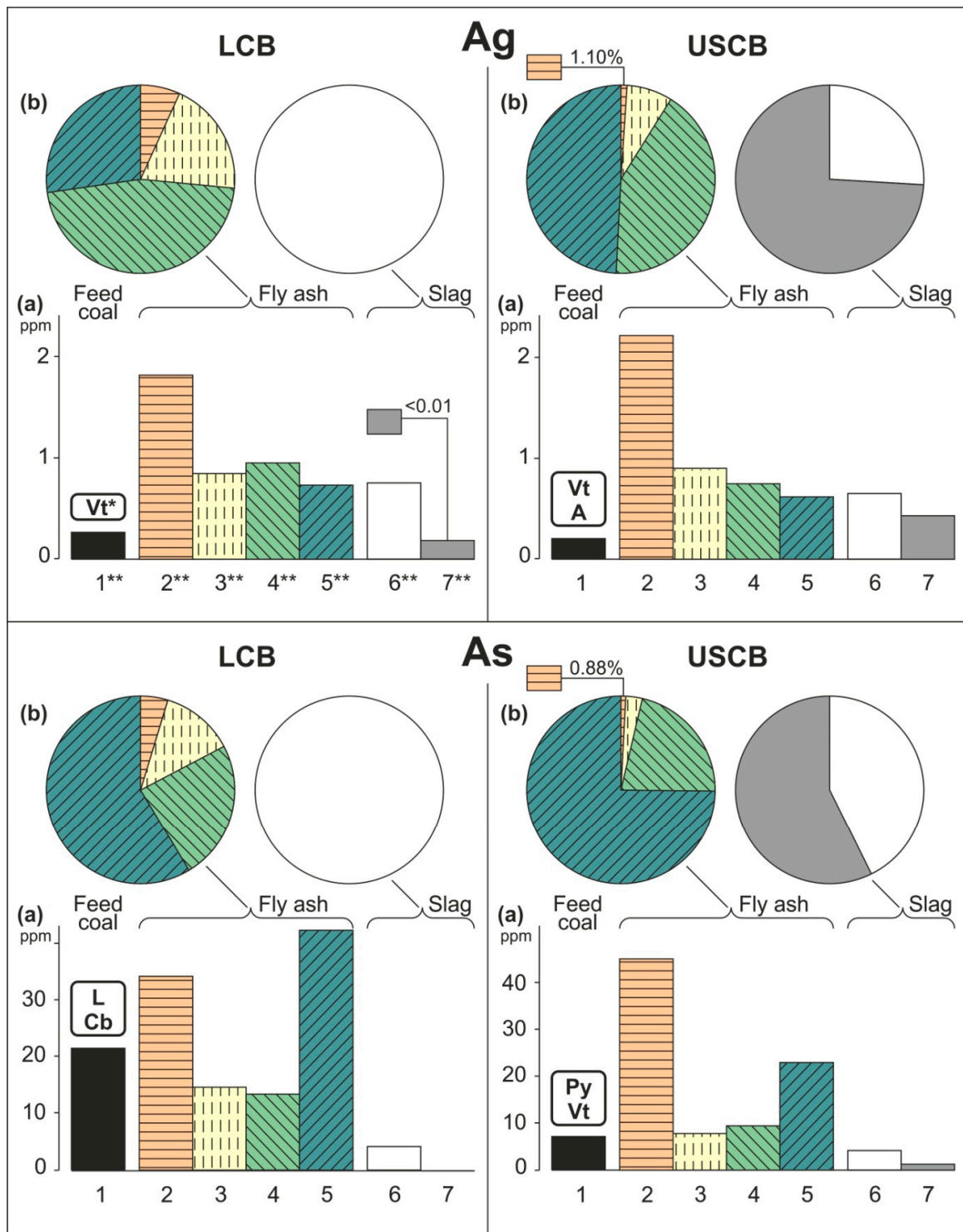


Figure 3. Cont.

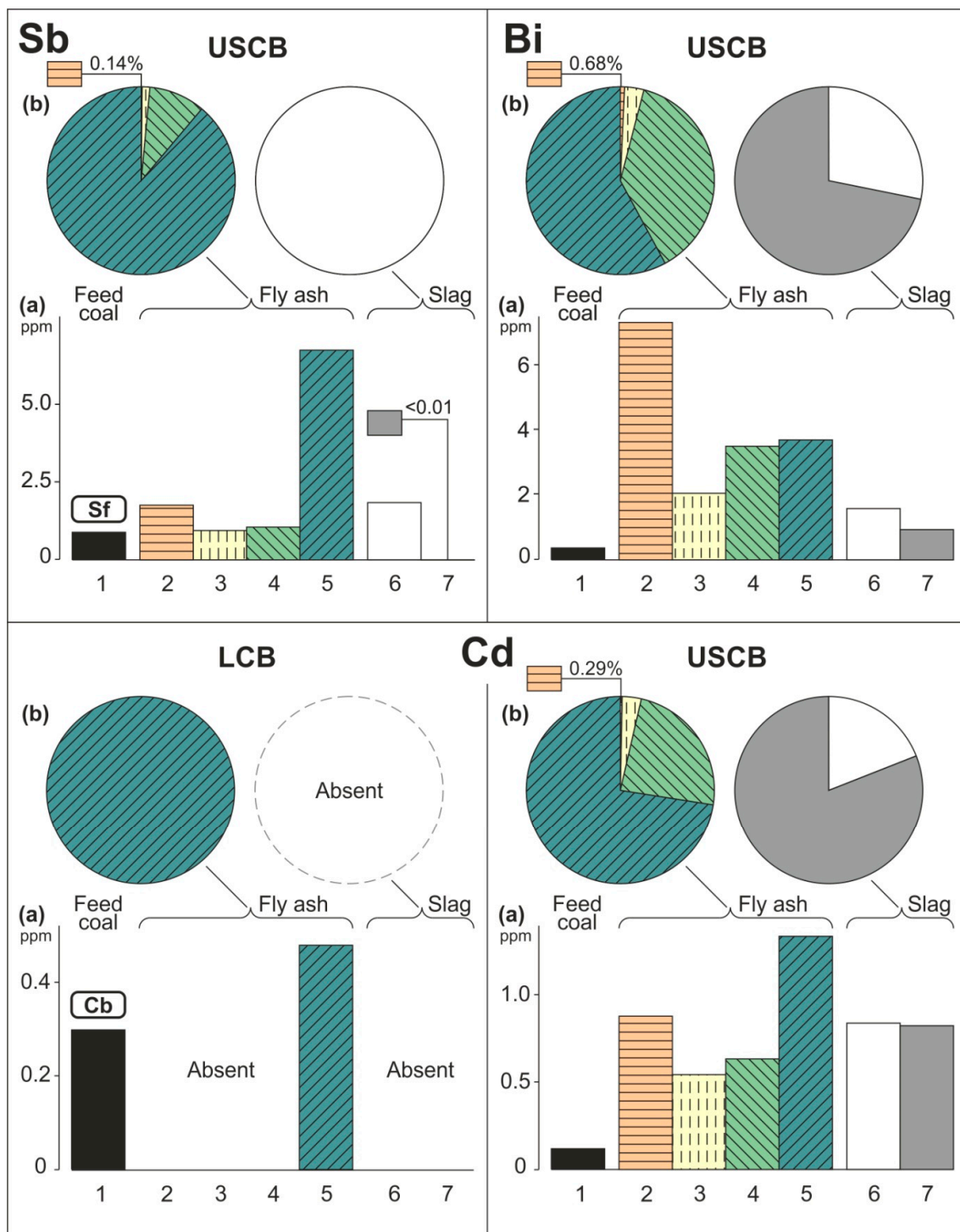


Figure 3. Cont.

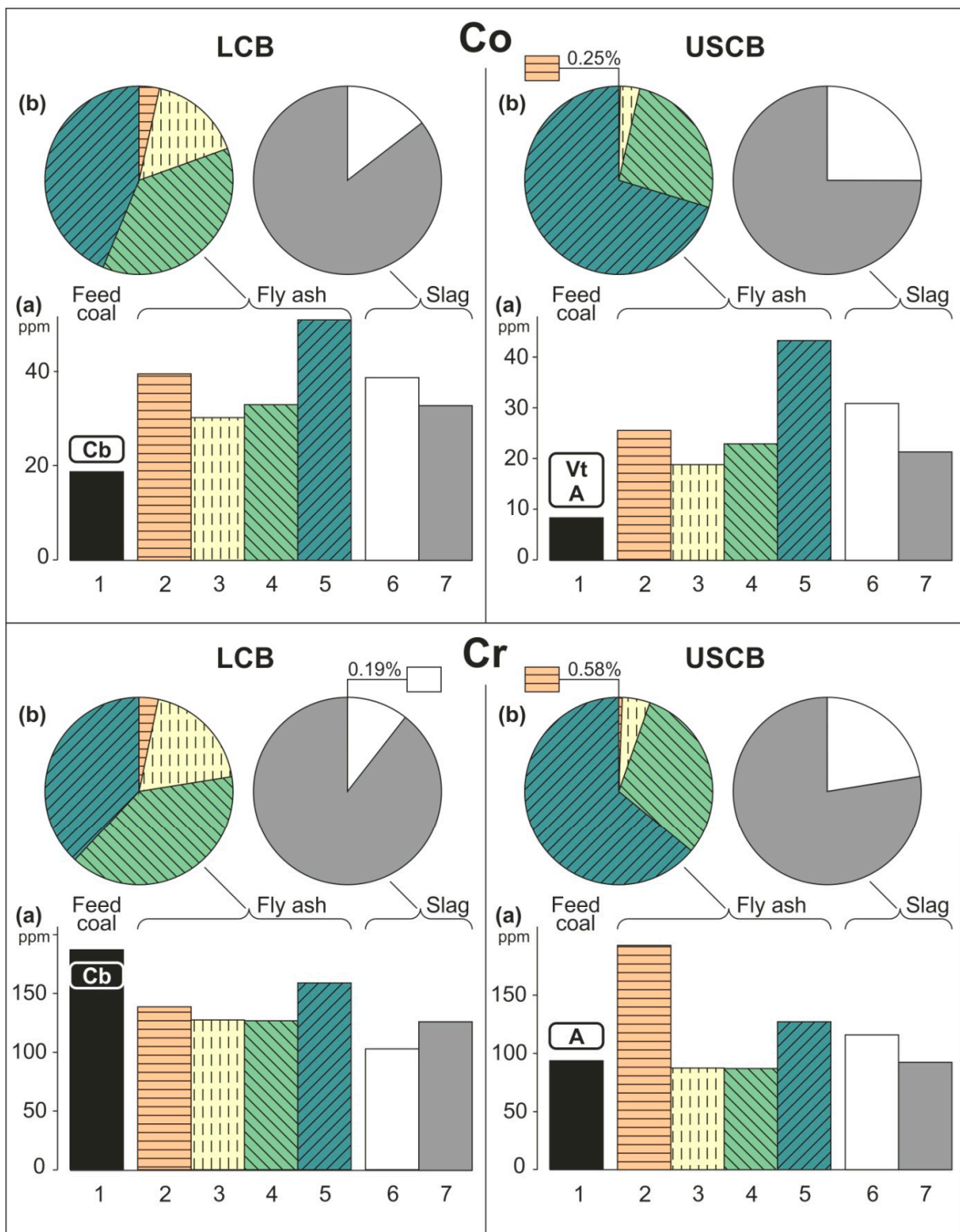


Figure 3. Cont.

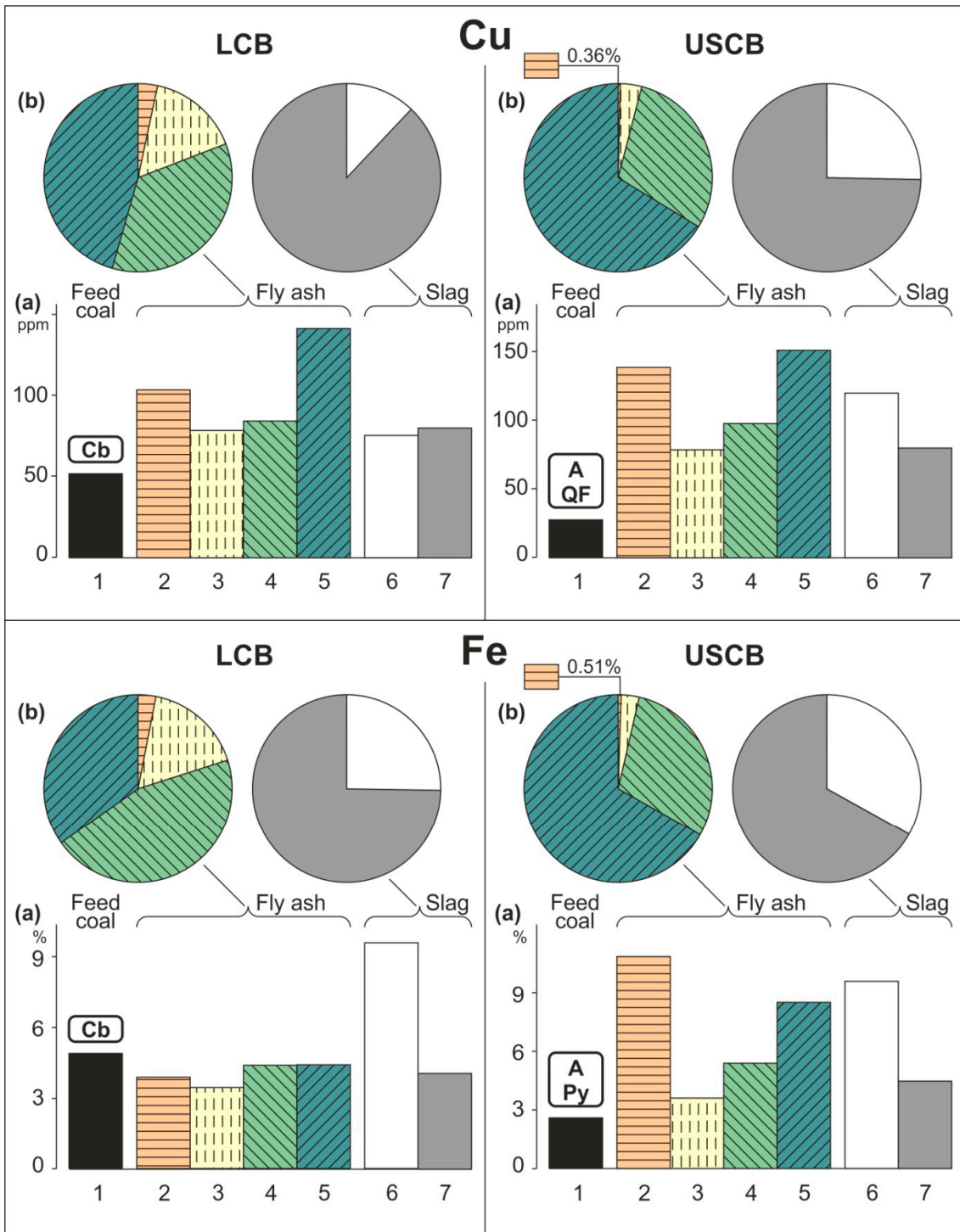


Figure 3. Cont.

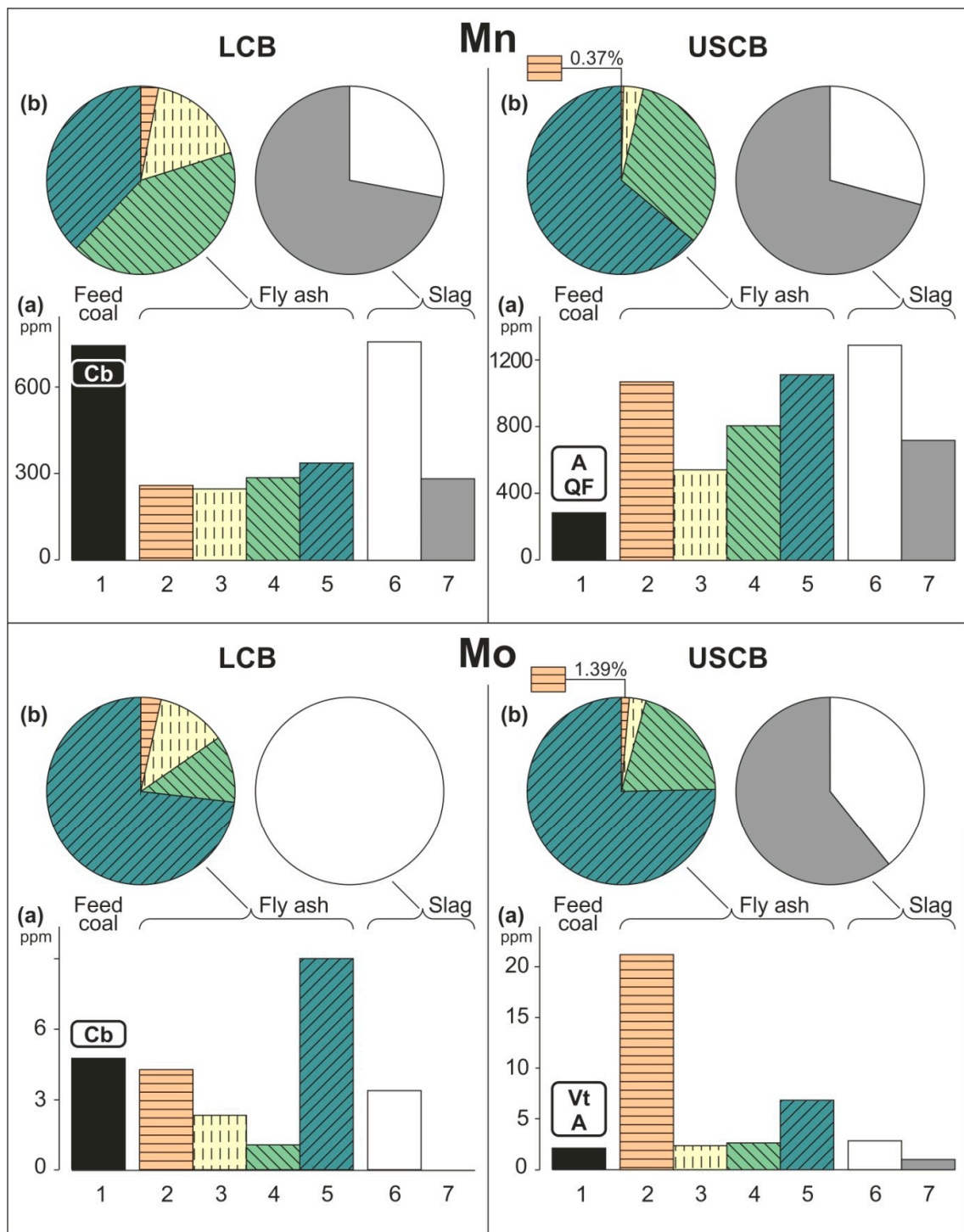


Figure 3. Cont.

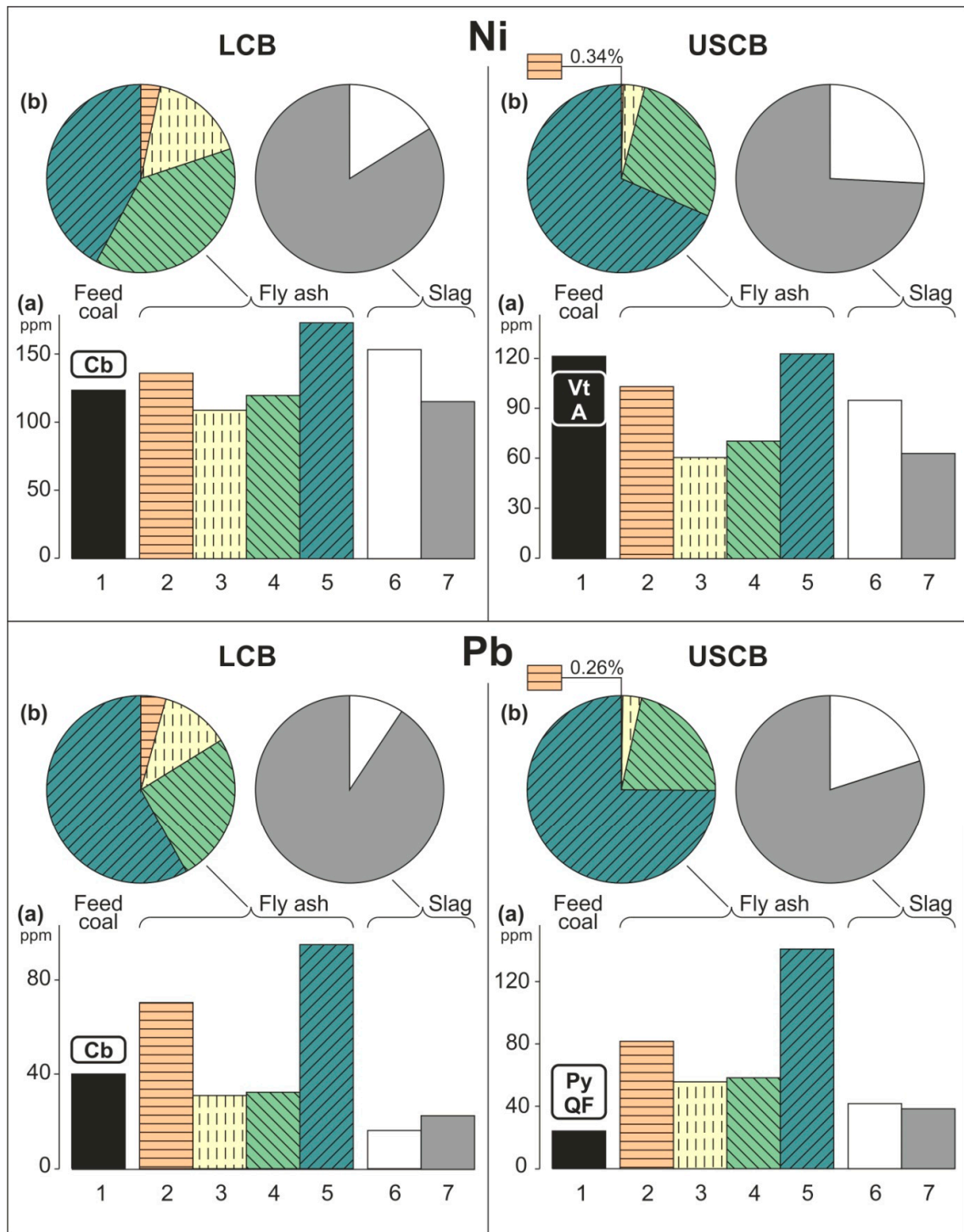


Figure 3. Cont.

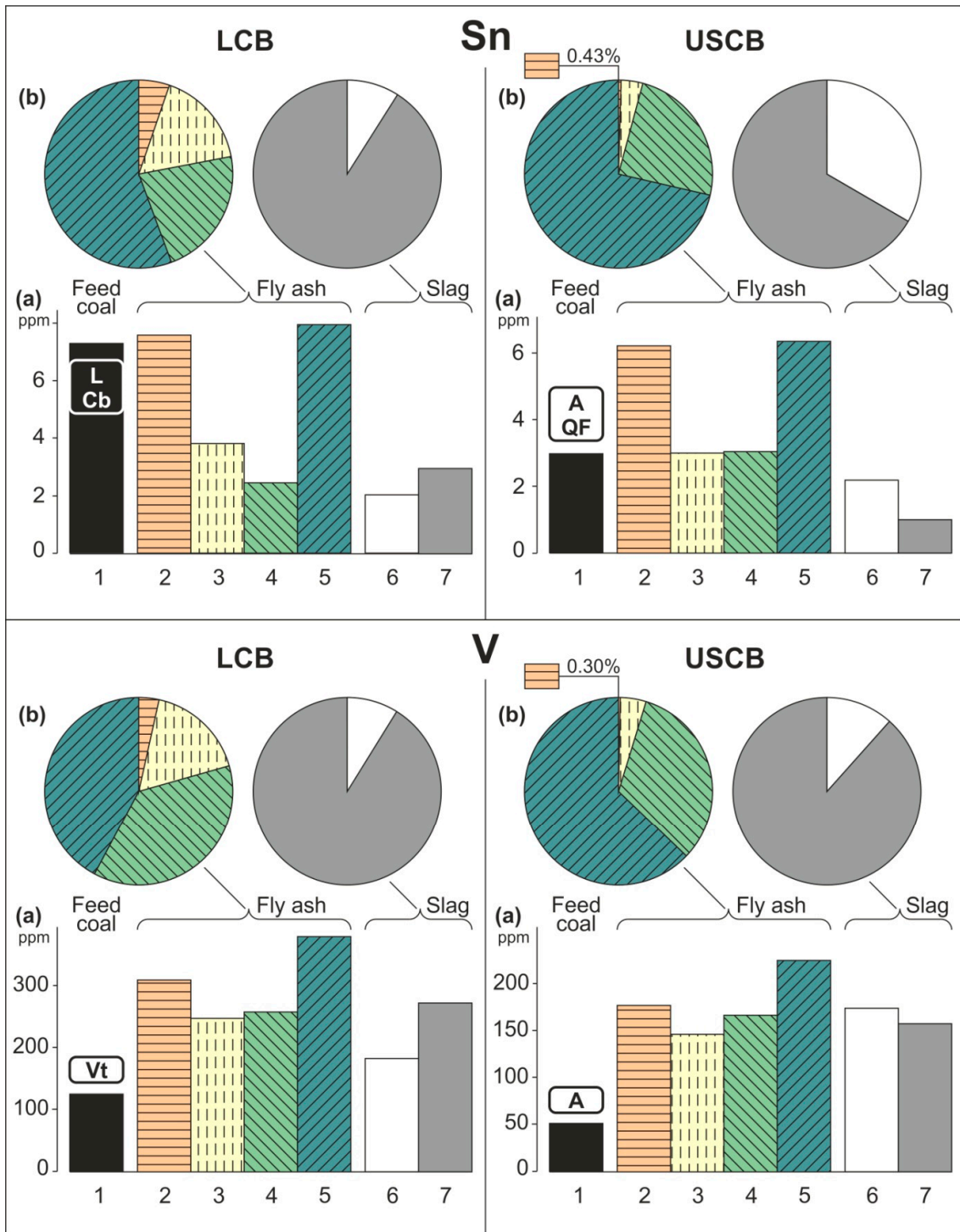


Figure 3. Cont.

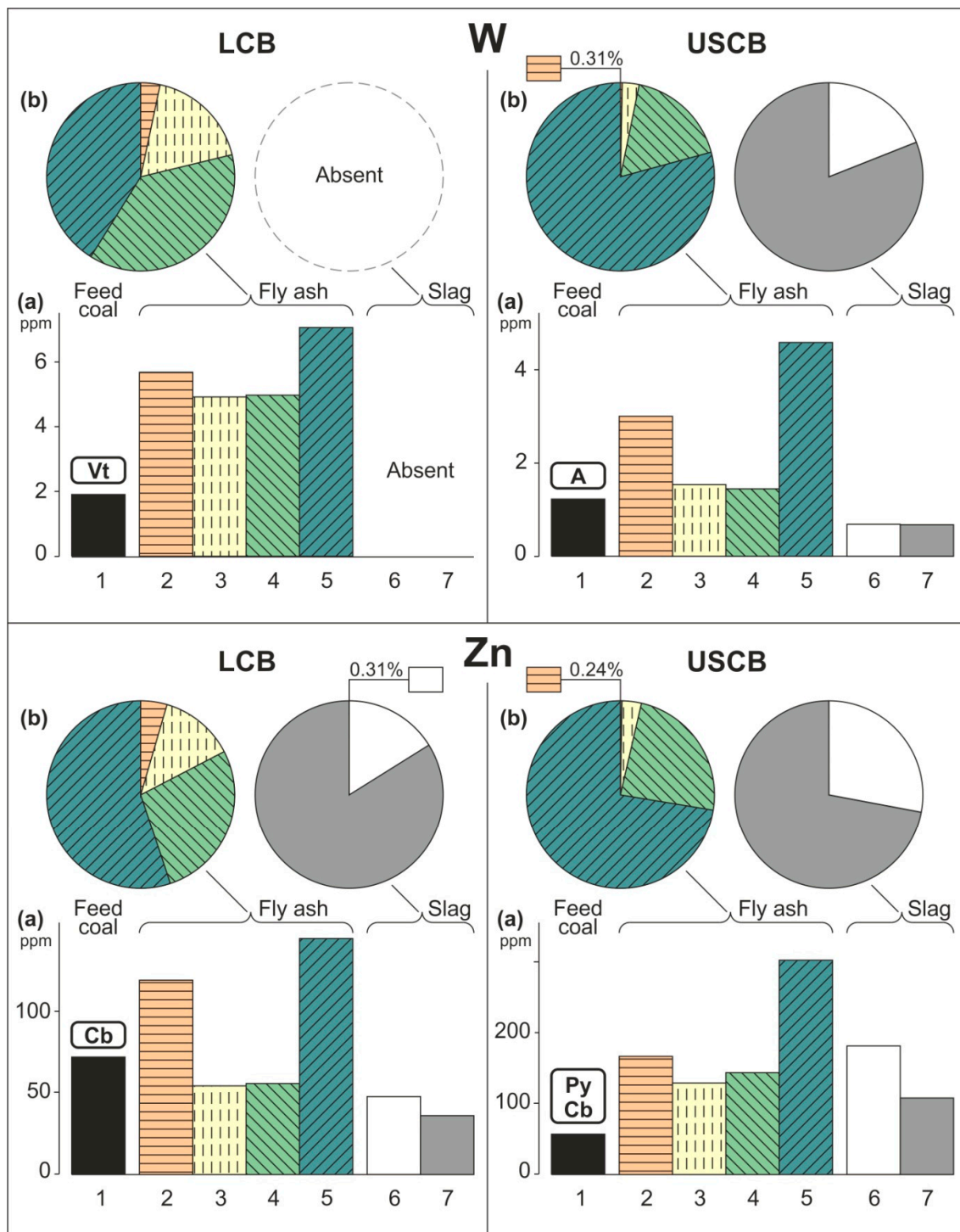


Figure 3. The distribution of EE content in the feed coal from the LCB and USCB and in the fly ash and slag (a), and their proportion in determining the average element concentration in fly ash and slag (b) (see Supplementary Materials Table S13). * Mode of occurrence of elements (Vt-vitrinite, L-liptinite, Cb-carbonate minerals, A-feed coal ash, Py-pyrite + marcasite, Sf-sulphate minerals, and QF-quartz+feldspars1), ** 1-feed coal, 2 ÷ 5 fly ash (grain with diameter: 2 -> 0.5 mm, 3 - 0.5 ÷ 0.2 mm, 4 - 0.2 ÷ 0.05 mm, 5 -< 0.05 mm), 6 ÷ 7 slag (6-magnetite, 7-nonmagnetite fraction).

4. Conclusions

1. A greater content of Ag, As, Co, Cr, Cu, Mn, Mo, Ni, Pb, Sn, V, W, and Zn, as well as a similar or lower content of Bi, Cd, and Sb, in feed coals than hard-coal Clarke values was found in the fuels burned in Poland. It is believed that, in feed coals from the LCB, elements such as As, Cd, Co, Cr, Cu, Fe, Mn, Mo, Ni, Pb, Sn, and Zn are probably bound to carbonate minerals; Ag, As, Sn, V, and W are bound to vitrinite or liptinite; Sn is bound to sulphate minerals only, while As and Sn to ash from feed coals (i.e., with generally organic and generally mineral matter). On the other hand, in the USCB coal feeds, Ag, As, Co, Mo, and Ni are probably bound to vitrinite, Fe, Pb, and Zn to pyrite with marcasite, to carbonates only Zn, to sulphate minerals only Sb, and to ash feed coals: Ag, Co, Cr, Cu, Fe, Mn, Mo, Ni, Sn, V, and W. The highest EE contents in feed coals from the LCB were found in siderite (As, Bi, Co, Cu, Fe, Mn, Pb, Sb, Sn, and V), pyrite with marcasite (Ag, Cd, Mo, Ni, and Zn) and clay minerals (Cr), and in feed coals from the USCB—in siderite and ankerite (Bi, Cu, Mn, Pb, Sb, and V), organic matter (Ag, As, Cd, W, and Zn), magnetite (Co, Fe, and Ni), clay minerals (Cr and Sn), and in pyrite with marcasite (Mo).
2. Compared to feed coals, the elements strongly enriched in fly ash resulting from its combustion from the LCB are Ag, Co, Cu, V, and W, and the coal constituting the feed coals from the USCB is Ag, As, Bi, Cd, Co, Cu, Fe, Mn, Mo, Pb, Sb, V, W, and Zn. Elements strongly enriched in slag are V (LCB) and Ag, Bi, Cd, Co, Cu, Fe, Mn, V, and Zn (the USCB). Elements depleted or absent in fly ash are Bi, Cd, Cr, Fe, Mn, Mo, Sb, and Sn (the LCB), and in slag they are Ag, As, Bi, Cd, Cr, Fe, Mn, Mo, Ni, Pb, Sb, Sn, W, and Zn (the LCB) and As, Mo, Sb, Sn, and W (the USCB).
3. The highest content of Cd, Co, Cu, Mn, Ni, Pb, Sn, V, W, and Zn in fly ash from combustion of feed coals from the LCB and the USCB, while As, Cr, Fe, and Mo in fly ash from combustion of feed coals from the LCB was found in concentrates of fly ash particles <0.05 mm thick in magnetite skeletal and Al-Si sphere. This group of particles also has the greatest impact on the average content of these elements in whole fly ash. The highest content of remaining elements in fly ash from the LCB (Ag) and from the USCB (Ag, As, Bi, Cr, Fe, and Mo) was recorded in the group of particles > 0.05 mm enriched in Al-Si sphere and crassisphere. The largest influence on the content of these elements in whole fly ash have particles of 0.05 mm –0.2 mm or < 0.05 mm. The highest content of most elements in the slag resulting from the combustion of coal feeds from the LCB (Co, Fe, Mn, Ni, and Zn) and from the USCB (Ag, As, Bi, Cd, Co, Cr, Fe, Mn, Ni, Pb, Sn, V, W, and Zn) were found in the magnetic fraction of slag, and the non-magnetic fraction has the greatest impact on the content of these elements in the whole slag. The magnetic content has the highest content and the largest impact on the content of some EE in the entire slag from the combustion of feed coals from the LCB (Ag, As, and Mo) and the USCB (Mo and Sb). On the other hand, the non-magnetic fraction has the highest content and the largest impact on the content of Cr, Cu, Pb, Sn, and V in the whole slag from the combustion of feed coals from the LCB. Fly ash and slag produced in power plants are considered neutral for the soil environment, due to their content EE.
4. It is assumed that there is a relationship between the binding mode of EE in feed coals and the distribution of EE in fly ash and slag.
 - 4.1. When coal feeds are burned, containing elements probably associated partly or exclusively with vitrinite and/or liptinite and partly or exclusively with organic matter, then we get the following:
 - Fly ash particles > 0.5 mm have the highest contents of Ag (coal feeds from the LCB and USCB), As, Bi, Cr, Fe, and Mo (feed coals from the USCB);
 - Co, Cr, Cu, Mn, Mo, and Ni condense more intensively in fly ash (feed coals from the USCB) than when these elements are bound only to carbonate minerals (feed coals from the LCB);

- Fly ash and slag particles are strongly enriched in elements (V and W) with a high melting point.
- 4.2. When coal feeds are burned in which EE are probably bound to carbonate minerals (feed coals from the LCB: Cd, Co, Cr, Cu, Fe, Mn, Mo, Ni, Pb, and Zn) and/or with sulphate minerals (feed coals from the USCB: Sb) and/or with pyrite with marcasite (feed coals from the USCB: Cd, Pb, and Zn), then the highest content of elements occurs in fly ash particles <0.05 mm, and these particles have the greatest impact on the content of elements in the whole fly ash.
 - 4.3. When coal feeds are burned, in which EE are probably bound, among others to pyrite with marcasite (USCB coal feeds: Cd, Fe, Pb, and Zn), then the enrichment of elements in fly ash is greater than when the elements in coal feeds (from the LCB) are bound to carbonate minerals.

Supplementary Materials: The following are available online at <http://www.mdpi.com/1996-1073/13/5/1131/s1>, Table S1: Sampling locations; Table S2: Results of reflected microscopic analysis; Table S3: X-ray diffractometric analysis results; Table S4: Separation efficiency for fly ash and slag; Table S5: Content of elements in coal ash samples; Table S6: Content of elements in samples feed coal; Table S7: SEM analysis results; Table S8: Results used to calculate the Pearson correlation coefficient; Table S9: Pearson correlation coefficient values; Table S10: Content of elements in samples fly ash and slag; Table S11: Arithmetic average of the elements content in feed coal; Table S12: Enrichment factor calculations; Table S13: Summary of the results of elements occurrence in coal and elemental distribution in fly ash and slag, and their contribution to determining the average content of elements in combustion residues.

Author Contributions: Conceptualization, H.R.P.; methodology, H.R.P.; formal analysis, L.R. and H.R.P.; investigation, H.R.P.; writing, H.R.P.; translation, L.R. All authors have read and agreed to the published version of the manuscript.

Funding: This research received no external funding.

Acknowledgments: Padhraig Kennan (University College Dublin) and Magdalena Misz-Kennan (University of Silesia in Katowice) the author is grateful for help in translating the manuscript into English

Conflicts of Interest: The authors declare no conflicts of interest.

References

1. Dai, S.; Ren, D.; Chou, C.-L.; Finkelman, R.B.; Seregin, V.V.; Zhou, Y. Geochemistry of trace elements in Chinese coals. A review of abundances, genetic types, impact of human health, and industrial utilization. *Int. J. Coal Geol.* **2012**, *94*, 3–21. [[CrossRef](#)]
2. Izquierdo, M.; Querol, X. Leaching behaviour of elements from coal combustion fly ash: An overview. *Int. J. Coal Geol.* **2012**, *94*, 54–66. [[CrossRef](#)]
3. Finkelman, R.B.; Dai, S.; French, D. The importance of minerals in coal as the hosts of chemical elements: A review. *Int. J. Coal Geol.* **2019**, *212*, 103251. [[CrossRef](#)]
4. Kabata-Pendias, A. *Trace Elements of Soils and Plants*, 4th ed.; CRC Press: Boca Raton, FL, USA; Taylor & Francis Group: Milton Park, UK, 2011; p. 534.
5. Yudovich, Y.E.; Ketris, M.P. *Toxic Trace Elements in Coals*; Russian Academie of Sciences: Moscow, Russia, 2005; p. 655. (In Russian)
6. Zhao, L.; Dai, S.; Finkelman, R.B.; French, D.; Graham, I.T.; Yang, Y.; Li, J.; Yang, P. Leaching behavior of trace elements from fly ashes of five Chinese coal power plants. *Int. J. Coal Geol.* **2020**, *219*, 103381. [[CrossRef](#)]
7. Duffus, J.H. "Heavy metals"—A meaningless term? (IUPAC Technical Report). *Pure Appl. Chem.* **2002**, *74*, 793–807. [[CrossRef](#)]
8. Bhangare, R.C.; Ajmal, P.Y.; Sahu, S.K.; Pandit, G.G.; Puranik, V.D. Distribution of trace elements in coal and combustion residues from five thermal power plants in India. *Int. J. Coal Geol.* **2011**, *86*, 349–356. [[CrossRef](#)]
9. Finkelman, R.B.; Palmer, C.A.; Wang, P. Quantification of the modes of occurrence of 42 elements in coal. *Int. J. Coal Geol.* **2018**, *185*, 138–160. [[CrossRef](#)]
10. Guo, R.; Yang, J.; Liu, Z. Behavior of trace elements during pyrolysis of coal in a simulated drop-tube reactor. *Fuel* **2004**, *83*, 639–643. [[CrossRef](#)]

11. Hower, J.C.; Granite, E.J.; Mayfield, D.B.; Lewis, A.S.; Finkelman, R.B. Notes on contributions to the science of rare earth element enrichment in coal and coal combustion byproducts. *Minerals* **2015**, *6*, 32. [[CrossRef](#)]
12. Hower, J.C.; Dai, S.; Eskenazy, G. Distribution of Uranium and Other Radionuclides in Coal and Coal Combustion Products, with Discussion of Occurrences of Combustion Products in Kentucky Power Plants. *Coal Comb. Gasif. Prod.* **2016**, *8*, 44–53. [[CrossRef](#)]
13. Pan, J.; Zhou, C.-C.; Zhang, N.-N.; Liu, C.; Tang, M.-C.; Cao, S.-S. Arsenic in coal: Modes of occurrence and reduction via coal preparation—A case study. *Int. J. Coal Prep. Util.* **2018**. [[CrossRef](#)]
14. Xu, M.; Yan, R.; Zheng, C.; Oiao, Y.; Han, J.; Sheng, C. Status of trace element emission in a coal combustion process: A review. *Fuel Proc. Technol.* **2003**, *85*, 215–237. [[CrossRef](#)]
15. Zhang, J.; Han, C.-L.; Xu, Y.-Q. The release of the hazardous elements from coal in the initial stage of combustion process. *Fuel Proc. Technol.* **2003**, *84*, 121–133. [[CrossRef](#)]
16. Zhou, L.; Guo, H.; Wang, X.; Chu, M.; Zhang, G.; Zhang, L. Effect of occurrence mode of heavy metal elements in a low rank coal on volatility during pyrolysis. *Int. J. Coal Sci. Technol.* **2019**, *6*, 235–246. [[CrossRef](#)]
17. Sia, S.G.; Wan, H.A. Enrichment of arsenic, lead, and antimony in Balingian coal from Sarawak, Malaysia: modes of occurrence, origin, and partitioning behaviour during coal combustion. *Int. J. Coal Geol.* **2012**, *101*, 1–15. [[CrossRef](#)]
18. Huang, Y.; Jin, B.; Zhong, Z.; Xiao, R.; Tang, Z.; Ren, H. Trace elements (Mn, Cr, Pb, Se, Zn, Cd and Hg) in emissions from a pulverized coal boiler. *Fuel Proc. Technol.* **2004**, *86*, 23–32. [[CrossRef](#)]
19. Linak, W.P.; Wendt, J.O.L. Toxic metal emissions from incineration: Mechanisms and control. *Prog. Energy Combust. Sci.* **1993**, *19*, 145–185. [[CrossRef](#)]
20. Querol, X.; Fernández-Turiel, J.L.; López-Soler, A. Trace elements in coal and their behavior during combustion in a large power station. *Fuel* **1995**, *74*, 331–343. [[CrossRef](#)]
21. Sekine, Y.; Sakajin, K.; Kikuchi, E. Release behavior of trace elements from coal during high-temperature processing. *Powder Technol.* **2008**, *180*, 210–215. [[CrossRef](#)]
22. Zhao, S.; Duan, Y.; Li, Y.; Liu, M.; Lu, J.; Ding, Y.; Gu, X.; Tao, J.; Du, M. Emission characteristic and transformation mechanism of hazardous trace elements in a coal-fired power plant. *Fuel* **2018**, *214*, 597–606. [[CrossRef](#)]
23. Bartoňová, L.; Raclavská, H.; Čech, B.; Kucbel, M. Behavior of Pb during coal combustion: An overview. *Sustainability* **2019**, *11*, 6061. [[CrossRef](#)]
24. Chen, G.; Sun, Y.; Wang, Q.; Yan, B.; Cheng, Z.; Ma, W. Partitioning of trace elements in coal combustion products: A comparative study of different applications in China. *Fuel* **2019**, *240*, 31–39. [[CrossRef](#)]
25. Cui, W.; Meng, Q.; Feng, Q.; Zhou, L.; Cui, Y.; Li, W. Occurrence and release of cadmium, chromium, and lead from stone coal combustion. *Int. J. Coal Sci Technol.* **2019**, *6*, 586–594. [[CrossRef](#)]
26. Dai, S.; Zhao, L.; Peng, S.; Chou, C.-L.; Wang, X.; Zhang, Y.; Li, D.; Sun, Y. Abundances and distribution of minerals and elements in high-alumina coal fly ash from the Jungar Power Plant, Inner Mongolia, China. *Int. J. Coal Geol.* **2010**, *81*, 320–332. [[CrossRef](#)]
27. Vejahati, F.; Xu, Z.; Gupta, R. Trace elements in coal: Associations with coal and minerals and their behaviour during coal utilization—A review. *Int. J. Coal Geol.* **2010**, *14*, 904–911. [[CrossRef](#)]
28. Wang, J.; Yang, Z.; Quin, S.; Panchal, B.; Sun, Y.; Niu, H. Distribution characteristics and migration patterns of hazardous trace elements in coal combustion products of power plants. *Fuel* **2019**, *258*, 116062. [[CrossRef](#)]
29. Duan, P.; Wang, W.; Liu, X. Distribution of As, Hg and other trace elements in different size and density fractions of the Reshuihe high-sulfur coal, Yunnan Province, China. *Int. J. Coal Geol.* **2017**, *173*, 129–141. [[CrossRef](#)]
30. Duan, P.; Wang, W.; Sang, S.; Qian, F.; Shao, P.; Zhao, X. Partitioning of hazardous elements during preparation of high-uranium coal from Rongyang, Guizhou, China. *J. Geochem. Explor.* **2018**, *185*, 81–92. [[CrossRef](#)]
31. Duan, P.; Wang, W.; Sang, S.; Tang, Y.; Ma, M.; Zhang, W.; Liang, B. Geochemistry of toxic elements and their removal via the preparation of high-uranium coal in Southwestern China. *Minerals* **2018**, *8*, 83. [[CrossRef](#)]
32. Duan, P.; Wang, W.; Sang, S.; Ma, M.; Wang, J.; Zhang, W. Modes of occurrence and removal of toxic elements from high uranium coals of Rongyang Mine by stepped release flotation. *Energy Sci. Eng.* **2019**, *7*, 1–9. [[CrossRef](#)]
33. Dai, S.; Yan, X.; Ward, C.R.; Hower, J.C.; Zhao, L.; Wang, X.; Zhao, L.; Ren, D.; Finkelman, R.B. Valuable elements in Chinese coals: A review. *J. Int. Geol. Rev.* **2018**, *60*, 590–620. [[CrossRef](#)]

34. Hower, J.C.; Dai, S.; Seredin, V.V.; Zhao, L.; Kostova, I.J.; Silva, L.F.O.; Mardon, S.M.; Gurdal, G. A note on the occurrence of yttrium and rare earth elements in coal combustion products. *Coal Comb. Gasific. Prod.* **2013**, *5*, 39–47.
35. Hower, J.C.; Qian, D.; Briot, N.J.; Henke, K.R.; Hood, M.M.; Taggart, R.K.; Hsu-Kim, H. Rare earth element associations in the Kentucky State University stoker ash. *Int. J. Coal Geol.* **2018**, *189*, 75–82. [[CrossRef](#)]
36. Hower, J.C.; Groppo, J.G.; Joshi, P.; Preda, D.V.; Gamliel, D.P.; Mohler, D.T.; Wisema, J.D.; Hopps, S.D.; Morgan, T.D.; Beers, T.; et al. Distribution of Lanthanides, Yttrium, and Scandium in the Pilot-Scale Beneficiation of Fly Ashes Derived from Eastern Kentucky Coals. *Minerals* **2020**, *10*, 105. [[CrossRef](#)]
37. King, J.F.; Taggart, R.K.; Smith, R.C.; Hower, J.C.; Hsu-Kim, H. Aqueous acid and alkaline extraction of rare earth elements from coal combustion ash. *Int. J. Coal Geol.* **2018**, *195*, 75–83. [[CrossRef](#)]
38. Drobek, L.; Michalik, B. Monitoring of the properties of energy waste subjected to recovery in underground excavations. *Wiad. Gór.* **2008**, *59*, 349–360. (In Polish)
39. Makowska, D.; Wierońska, F.; Dziok, T.; Strugała, A. Ecotoxic elements emission from the combustion of solid fuels due to legal regulations. *Energy Policy J.* **2017**, *20*, 89–102. (In Polish)
40. Makowska, D.; Strugała, A.; Wierońska, F.; Baciór, M. Assessment of the content, occurrence, and leachability of arsenic, lead, and thallium in wastes from coal cleaning processes. *Environ. Sci. Pollut. Res.* **2018**, *26*, 8418–8428. [[CrossRef](#)]
41. Ratajczak, T.; Gawęł, A.; Górniak, K.; Muszyński, M.; Szydłak, T.; Wyszomirski, P. Characteristics of fly ash from combustion of some hard and brown coals. *Spec. Pap. Mineral. Soc. Pol.* **1999**, *15*, 34. (In Polish)
42. Parzenty, H.R.; Róg, L. The role of mineral matter in concentrating uranium and thorium in coal and combustion residues from power plant in Poland. *Minerals* **2019**, *9*, 312. [[CrossRef](#)]
43. Smołka-Danielowska, D. *The X-Ray Structure Analysis of Amorphous and Nanocrystalline Materials*; Printing House, WW; Earth Science, Series; Jankowski, A., Ed.; University of Silesia: Katowice, Poland, 2013; p. 112. (In Polish)
44. ISO 7404-3. *Methods for the Petrographic Analysis of Bituminous Coal and Anthracite—Part 3: Method of Determining Maceral Group Composition*; International Organization for Standardization: Geneva, Switzerland, 2009; p. 7.
45. ISO 7404-5. *Methods for the Petrographic Analysis of Bituminous Coal and Anthracite—Part 5: Method of Determining Microscopically the Reflectance of Vitrinite*; International Organization for Standardization: Geneva, Switzerland, 2009; p. 14.
46. Taylor, J.C. Computer programs for standardless quantitative analysis of minerals using the full powder diffraction profile. *Powder Diffr.* **1991**, *6*, 2–9. [[CrossRef](#)]
47. Rietveld, H.M. A profile refinement method for nuclear and magnetic structures. *J. Appl. Crystallogr.* **1969**, *2*, 65–71. [[CrossRef](#)]
48. Ruan, C.-D.; Ward, C.R. Quantitative X-ray powder diffraction analysis of clay minerals in Australian coals using Rietveld methods. *Appl. Clay Sci.* **2002**, *21*, 227–240. [[CrossRef](#)]
49. Mahieux, P.Y.; Aubert, J.E.; Cyr, M.; Coutand, M.; Hussosn, B. Quantitative mineralogical composition of complex mineral wastes—Contribution of the Rietveld method. *Waste Manag.* **2010**, *30*, 378–388. [[CrossRef](#)] [[PubMed](#)]
50. PN-ISO 1171:2002-Polish Version. *Solid Fuels-Ash Determination*; Polish Standardization Committee: Warsaw, Poland, 2002.
51. Bureau Veritas Mineral Laboratories Schedule of Services Bro. Vancouver, Canada, 2020. Available online: <http://acmelab.com> (accessed on 2 January 2020).
52. Economic Commission for Europe; Committee on Sustainable Energy. *International Classification of in-Seam Coals*; United Nations Report Energy/1998/19; UN: New York, NY, USA; Geneva, Switzerland, 1998.
53. Vassilev, S.V.; Vassileva, C.G.; Karayigit, A.I.; Bulut, Y.; Alastuey, A.; Querol, X. Phase-mineral and chemical composition of composite samples from feed coals, bottom ashes and fly ashes at the Soma power station, Turkey. *Int. J. Coal Geol.* **2005**, *61*, 35–63. [[CrossRef](#)]
54. Vassileva, C.G.; Vassilev, S.V. Behaviour of inorganic matter during heating of Bulgarian coals. 2. Subbituminous and bituminous coals. *Fuel Proc. Technol.* **2006**, *87*, 1095–1116. [[CrossRef](#)]
55. Vassilev, S.V.; Eskenazy, G.N.; Vassileva, C.G. Behaviour of elements and minerals during preparation and combustion of the Pernik coal, Bulgaria. *Fuel Proc. Technol.* **2001**, *72*, 103–129. [[CrossRef](#)]

56. Asuen, G.O. Elemental concentration and their relationship in Howick Coal Group, England. *Chem. Erde* **1988**, *48*, 321–332.
57. Dai, S.; Hou, X.; Ren, D.; Tang, Y. Surface analysis of pyrite in the No. 9 coal seam, Wuda Coalfield, Inner Mongolia, China, using high-resolution time-of-flight secondary ion mass-spectrometry. *Int. J. Coal Geol.* **2003**, *55*, 139–150. [[CrossRef](#)]
58. Deditius, A.P.; Utsunomiya, S.; Reich, M.; Kesler, S.E.; Ewing, R.C.; Hough, R.; Walshe, J. Trace metal nanoparticles in pyrite. *Ore Geol. Rev.* **2011**, *42*, 32–46. [[CrossRef](#)]
59. Kolker, A. Minor element distribution in iron disulfides in coal: A geochemical review. *Int. J. Coal Geol.* **2012**, *94*, 32–43. [[CrossRef](#)]
60. Parzenty, H.R.; Róg, L. Modes of occurrence of ecotoxic elements in coal from the Upper Silesian Coal Basin, Poland. *Arab. J. Geosci.* **2018**, *11*, 790. [[CrossRef](#)]
61. Wiese, R.G.; Muir, I.J.; Fyfe, W.S. Trace-element siting in iron sulphides in Ohio coals determined by secondary ion mass spectrometry (SIMS). *Int. J. Coal Geol.* **1990**, *14*, 155–174. [[CrossRef](#)]
62. Dai, S.; Bechtel, A.; Eble, C.F.; Flores, R.M.; French, D.; Graham, I.T.; Hood, M.M.; Hower, J.C.; Korasidis, V.A.; Moore, T.A.; et al. Recognition of peat depositional environments in coal: A review. *Int. J. Coal Geol.* **2020**, *219*, 103383. [[CrossRef](#)]
63. Mukherjee, K.N.; Dutta, N.R.; Chandra, E.; Pandalai, H.S.; Singh, M.P. A statistical approach to the study of the distribution of trace elements and their organic/inorganic affinity in Lower Gondwana Coals of India. *Int. J. Coal Geol.* **1988**, *10*, 99–108. [[CrossRef](#)]
64. Zubovic, P.; Stadnichenko, T.; Sheffey, N.B. Distribution of minor elements in coal beds of the Eastern Interior Region. *Geol. Surv. Bul.* **1964**, *1117*, 1–41.
65. Ketris, M.P.; Yudinich, Y.E. Estimations of Clarkes for Carbonaceous biolithes: World averages for trace element contents in black shales and coals. *Int. J. Coal Geol.* **2009**, *78*, 135–148. [[CrossRef](#)]
66. Bojakowska, I.; Pasieczna, A. Arsenic and antimony in bituminous and brown coal from Polish deposits. *Environ. Prot. Nat. Resour.* **2007**, *31*, 522–526. (In Polish)
67. Cebulak, S. Determination of geochemical components of coal from the point of view of full utilization and environmental preservation. In *Geological Problems of Coal Basins in Poland*; Bojkowski, K., iPorzycki, K., Eds.; Geological Institute: Warsaw, Poland, 1983; pp. 335–361.
68. Hanak, B.; Kokowska-Pawłowska, M. Variability of the content of the trace elements in the associated rocks and coal ashes from the coal seams 620. *Sci. Pap. Sil. Univ. Technol.* **2004**, *260*, 155–165. (In Polish)
69. Marczak, M.; Parzenty, H. Geochemical and ecological evaluation of Pb-enriched coals from the Chełm deposit. *Przeg. Geol* **1985**, *33*, 680–683. (In Polish)
70. Marczak, M.; Parzenty, H. Concentration of cadmium as a criterion in ecological evaluation of coals from the Chełm deposit (Lublin Coal Basin). *Przeg. Geol* **1989**, *37*, 272–275. (In Polish)
71. Parzenty, H.R. Silver, tin and tungsten in the Lublin Formation coal (Westphal B) in the Lublin Coal Basin (LZW). *Gosp. Sur. Miner* **2009**, *25*, 147–167. (In Polish)
72. Parzenty, H.R.; Róg, L. Geochemical characteristics of the bismuth and antimony occurrence in some coal seams in the Lublin Coal Basin (LCB). *Arch. Min. Sci.* **2017**, *62*, 313–324. [[CrossRef](#)]
73. Ptak, B.; Rózkowska, A. *Geochemical Atlas of Coal Deposits Upper Silesian Coal Basin*; Publishing of Polish Geological Institute: Warszawa, Poland, 1995; p. 53.
74. Parzenty, H. The role of mineral substance in formation of zinc, lead and cadmium contents in the eastern part of the Upper Silesian Coal Basin. *Przeg. Górn* **1990**, *46*, 16–19. (In Polish)
75. Parzenty, H.R. *The Influence of Inorganic Mineral Substances on Content of Certain Trace Elements in the Coal of the Upper Silesian Coalfield*; Scientific Papers of Silesian University in Katowice No. 1460 Earth Science; Jankowski, T., Ed.; University of Silesia Publishing House: Katowice, Poland, 1995; p. 90.
76. Marczak, M. *Genesis and Regularities of the Trace Elements Occurrence in the Chełm Coal Deposit at Coal Basin of Lublin*; Scientific Papers of Silesian University in Katowice; Jachowicz, A., Konstatynowicz, E., Eds.; University of Silesia Publishing House: Katowice, Poland, 1985; Volume 748, p. 109.
77. Parzenty, H. Lead distribution in coal and coaly shales in the Upper Silesian Coal Basin. *Geol. Quarterly* **1994**, *38*, 43–58.
78. Parzenty, H.R.; Róg, L. Evaluation the value of some petrographic, phisico-chemical and geochemical indicators of quality of coal in paralic series of the Upper Silesian Coal Basin and attempt to find a correlation between them. *Gosp. Sur. Miner.* **2017**, *33*, 51–76.

79. Parzenty, H.; Rózkowska, A. An influence of organic and inorganic matter on lead content in coals and coaly shales of the Upper Silesian Coal Basin. *Przeg. Geol* **1992**, *40*, 656–659. (In Polish)
80. Hill, P.A. Vertical distribution of elements in Deposit No. 1, Hat Creek, British Columbia: A preliminary study. *Int. J. Coal Geol* **1990**, *15*, 77–111. [[CrossRef](#)]
81. Parzenty, H. Differences in content and bonding pattern of certain elements in coal of the Upper Silesian Coal Basin throughout a single seam profile. *Przeg. Górń* **1989**, *45*, 17–21. (In Polish)
82. Chen, J.; Chen, P.; Yao, D.; Huang, W.; Tang, S.; Wang, W.; Liu, W.; Hu, Y.; Zhang, B.; Sha, J. Abundance, distribution, and modes of occurrence of uranium in Chinese Coals. *Minerals* **2017**, *7*, 239. [[CrossRef](#)]
83. Liu, C.; Zhou, C.; Zhang, N.; Pan, J.; Cao, S.; Tang, M.; Ji, W.; Hu, T. Modes of occurrence and partitioning behavior of trace elements during coal preparation—A case study in Guizhou Province, China. *Fuel* **2019**, *243*, 79–87. [[CrossRef](#)]
84. Makowska, D.; Bytnar, K.; Dziok, T.; Rozwadowska, T. Effect of coal cleaning on the content of some heavy metals in Polish bituminous coal. *Przem. Chem.* **2014**, *93*, 2048–2205.
85. Mohanty, M.K.; Honaker, R.Q.; Mondal, K.; Paul, B.C.; Ho, K. Trace element reductions in fine coal using advanced physical cleaning. *Coal. Prep.* **1998**, *19*, 195–211. [[CrossRef](#)]
86. Strugała, A.; Makowska, D.; Bytnar, K.; Rozwadowska, T. Analysis of the contents of selected critical elements in waste from the hard coal cleaning process. *Energy Policy J.* **2014**, *17*, 77–89. (In Polish)
87. Misz, M.A. Comparison of chars in slag and fly ash as formed in pf boilers from Będzin Power Station (Poland). *Fuel* **2002**, *81*, 1351–1358. [[CrossRef](#)]
88. Parzenty, H.R.; Róg, L. Distribution of heavy metals in fly ash originating from burning coal of Upper Silesian Coal Basin. *Przeg. Górń.* **2001**, *57*, 52–60. (In Polish)
89. Vassilev, S.V.; Menedez, R.; Diaz-Somoano, M.; Martinez-Tarazona, M.R. Phase-mineral and chemical composition of coal fly ashes as a basis for their multicomponent utilization. 2. Characterization of ceramic cenosphere and salt concentrates. *Fuel* **2004**, *83*, 585–603. [[CrossRef](#)]
90. Vassilev, S.V.; Menedez, R.; Borrego, A.G.; Diaz-Somoano, M.; Martinez-Tarazona, M.R. Phase-mineral and chemical composition of coal fly ashes as a basis for their multicomponent utilization. 3. Characterization of magnetic and char concentrates. *Fuel* **2004**, *83*, 1563–1583. [[CrossRef](#)]
91. Vassilev, S.V.; Menedez, R. Phase-mineral and chemical composition of coal fly ashes as a basis for their multicomponent utilization. 4. Characterization of heavy concentrates and improved fly ash residues. *Fuel* **2005**, *84*, 973–991. [[CrossRef](#)]
92. The Regulation of the Minister of the Environment of 1 September 2016 on the assessment of the pollution of the earth's surface. In *Polish Journal of Laws 2016 Item 1395*; The Regulation of the Minister of the Environment: Warsaw, Poland, 2016.
93. Sanjuán, M.A.; Quintana, B.; Argiz, C. Coal bottom ash natural radioactivity in building materials. *J. Radioanal. Nucl. Chem.* **2019**, *319*, 91–99. [[CrossRef](#)]
94. Szarek, Ł.M. The issue of the use of calcareous fly ash in concrete technology. *Arch. Waste Manag. Environ. Prot.* **2015**, *17*, 1–20.
95. The Regulation of the Minister of the Environment of 15 July 2011 on the criteria for the classification of extractive waste for inert waste. In *Polish Journal of Laws 2011 Item 1048*; The Regulation of the Minister of the Environment: Warsaw, Poland, 2011.
96. Directive 2006/21/EC of the European Parliament and of the Council of 15 March 2006 on the Management of Waste from Extractive Industries and Amending Directive 2004/35/EC. Available online: <http://www.legislation.gov.uk/eudr/2006/21/introduction> (accessed on 2 January 2020).
97. Tian, Q.; Guo, B.; Nakama, S.; Sasaki, K. Distributions and Leaching Behaviors of Toxic Elements in Fly Ash. *ACS Omega* **2018**, *3*, 13055–13064. [[CrossRef](#)] [[PubMed](#)]
98. Mazurek, R.; Kowalska, J.; Gasiorek, M.; Zadrożny, P.; Józefowska, A.; Zaleski, T.; Kępka, W.; Tymczuk, M.; Orłowska, K. Assessment of heavy metals contamination in surface layers of Roztocze National Park forest soils (SE Poland) by indices of pollution. *Chemosphere* **2017**, *168*, 839–850. [[CrossRef](#)] [[PubMed](#)]
99. Siwek, M. Plants in postindustrial sites, contaminated with heavy metals. Part I. Uptake, transport and toxicity of heavy (trace) metals. *Wiad. Botan* **2008**, *52*, 7–22. (In Polish)
100. Finkelman, R.B. Health Impacts of Coal: Facts and Fallacies. *J. Hum. Environ.* **2007**, *36*. [[CrossRef](#)]

101. Blaha, U.; Sapkota, B.; Appel, E.; Stanjek, H.; Rösler, W. Micro-scale grain-size analysis and magnetic properties of coal-fired power plant fly ash and its relevance for environmental magnetic pollution studies. *Atm. Environ.* **2008**, *42*, 8359–8370. [[CrossRef](#)]
102. Çayır, A.; Belivermiş, M.; Kılıç, O.; Coşkun, M. Heavy metal and radionuclide levels in soil around Afsin-Elbistan coal-fired thermal power plants, Turkey. *Environ. Earth Sci.* **2012**, *67*, 1183–1190. [[CrossRef](#)]
103. Huggins, F.; Goodarzi, F. Environmental assessment of elements and polyaromatic hydrocarbons emitted from a Canadian coal-fired power plant. *Int. J. Coal Geol.* **2009**, *77*, 282–288. [[CrossRef](#)]
104. Kisku, G.C.; Yadav, S.; Sharma, R.K.; Negi, M.P.S. Potential environmental pollution hazards by coal based power plant at Jhansi (UP) India. *Environ. Earth Sci.* **2012**, *67*, 2109–2120. [[CrossRef](#)]
105. Magiera, T.; Parzenty, H.R.; Róg, L.; Chybiorz, R.; Wawer, M. Spatial variation of soil magnetic susceptibility in relation to different emission sources in southern Poland. *Geoderma* **2015**, *255–256*, 94–103. [[CrossRef](#)]
106. Veneva, L.; Hoffmann, V.; Jordanova, D.; Jordanova, N.; Fehr, T. Rock magnetic, mineralogical and microstructural characterization of fly ashes from Bulgarian power plants and the nearby anthropogenic soils. *Phys. Chem. Earth* **2004**, *29*, 1011–1023. [[CrossRef](#)]
107. Parzenty, H.R. Differences between the content of selected ecotoxic elements in feed coal, combustion residues, soils and common beech (*Fagus sylvatica* L.) in the surrounded of the power plant in Poland. *SGEM Conf.* **2019**, *19*, 271–283.
108. Sanei, H.; Goodarzi, F.; Outridge, P.M. Spatial distribution of mercury and other trace elements in recent lake sediments from central Alberta, Canada: An assessment of the regional impact of coal-fired power plants. *Int. J. Coal Geol.* **2010**, *82*, 105–115. [[CrossRef](#)]
109. Turhan, S. Evaluation of agricultural soil radiotoxic element pollution around a lignite-burning thermal power plant. *Radiochim. Acta* **2019**, *108*, 77–85. [[CrossRef](#)]



© 2020 by the authors. Licensee MDPI, Basel, Switzerland. This article is an open access article distributed under the terms and conditions of the Creative Commons Attribution (CC BY) license (<http://creativecommons.org/licenses/by/4.0/>).